
SCALABLE FIRST-ORDER METHODS FOR ROBUST MDPs

Julien Grand-Clément
Columbia University
jg3728@columbia.edu

Christian Kroer
Columbia University
ck2945@columbia.edu

ABSTRACT

Robust Markov Decision Processes (MDPs) are a powerful framework for modeling sequential decision making problems with model uncertainty. This paper proposes the first first-order framework for solving robust MDPs. Our algorithm interleaves primal-dual first-order updates with approximate Value Iteration updates. By carefully controlling the tradeoff between the accuracy and cost of Value Iteration updates, we achieve an ergodic convergence rate of $O(A^2 S^3 \log(S) \log(\epsilon^{-1}) \epsilon^{-1})$ for the best choice of parameters on ellipsoidal and Kullback-Leibler s -rectangular uncertainty sets, where S and A is the number of states and actions, respectively. Our dependence on the number of states and actions is significantly better (by a factor of $O(A^{1.5} S^{1.5})$) than that of pure Value Iteration algorithms. In numerical experiments on ellipsoidal uncertainty sets we show that our algorithm is significantly more scalable than state-of-the-art approaches. Our framework is also the first one to solve robust MDPs with s -rectangular KL uncertainty sets.

1 Introduction

In this paper we focus on solving robust Markov Decision Processes (MDPs) with finite set of states and actions. Markov decision process models are widely used in decision-making [Bertsekas, 2007, Puterman, 1994]. In the classical MDP setting, for each state $s \in \mathbb{S}$, the decision maker chooses a probability distribution \mathbf{x}_s over the set of actions \mathbb{A} . The decision maker incurs a cost $\sum_{a=1}^{|\mathbb{A}|} x_{sa} c_{sa}$ for some non-negative scalars c_{sa} and then randomly enters a new state, according to transition kernels $\mathbf{y} = \{\mathbf{y}_{sa} \in \Delta(|\mathbb{S}|)\}_{sa}$ over the next state, where $\Delta(|\mathbb{S}|)$ is the simplex of size $|\mathbb{S}|$. Given a discount factor λ , the goal of the decision-maker is to minimize the infinite horizon discounted expected cost

$$C(\mathbf{x}, \mathbf{y}) = E^{\mathbf{x}, \mathbf{y}} \left[\sum_{t=0}^{\infty} \lambda^t c_{s_t a_t} \mid s_0 \sim p_0 \right].$$

The cost of a policy can be highly sensitive to the exact kernel parameters \mathbf{y} . We consider a robust approach where the uncertainty in \mathbf{y} is adversarially selected from an *uncertainty set* \mathbb{P} centered around a nominal estimation \mathbf{y}^0 of the true transition kernel. Our goal is to solve the *robust MDP* problem $\min_{\mathbf{x} \in \Pi} \max_{\mathbf{y} \in \mathbb{P}} C(\mathbf{x}, \mathbf{y})$ [Iyengar, 2005, Nilim and Ghaoui, 2005, Wiesemann et al., 2013, Goh et al., 2018, Goyal and Grand-Clement, 2018], which has found applications in healthcare [Steimle and Denton, 2017, Steimle et al., 2018, Goh et al., 2018, Grand-Clement et al., 2020]. We focus on s -rectangular uncertainty sets, where $\mathbb{P} = \times_{s \in \mathbb{S}} \mathbb{P}_s$, for $\mathbb{P}_s \subseteq \mathbb{R}_+^{|\mathbb{A}| \times |\mathbb{S}|}$, and solving the robust

MDP problem is equivalent to computing the fixed point of the *Bellman operator*, thus allowing a *value iteration* (VI) algorithm [Wiesemann et al., 2013].

We focus on two specific classes of s -rectangular uncertainty sets. *Kullback-Leibler* (KL) uncertainty sets are constructed from density estimation and naturally appear as approximations of the confidence intervals for the maximum likelihood estimates of \mathbf{y} given some historical transition data [Iyengar, 2005]. *Ellipsoidal* uncertainty sets are widely used because of their tractability and the probabilistic guarantees of the optimal solutions of the robust problems [Ben-Tal and Nemirovski, 2000, Bertsimas et al., 2019]. For ellipsoidal uncertainty sets, the value iteration algorithm involves solving a convex program with a quadratic constraint at every epoch. While this can be done in polynomial time with modern Interior Point Methods (IPMs, Lobo et al. [1998]), this requires inverting matrices at every step of the IPM which can be intractable for large MDP instances. Typically, for $S = |\mathbb{S}|, A = |\mathbb{A}|$, the complexity of VI to return an ϵ -solution to the robust MDP problem with ellipsoidal uncertainty sets is $O(A^{3.5} S^{4.5} \log^2(\epsilon^{-1}))$. This may prove prohibitive for large instances. For KL uncertainty sets, we are not aware of any tractable algorithm for solving s -rectangular robust MDP with KL uncertainty sets, even though they are well understood in Distributionally Robust Optimization [Hu and Hong, 2013].

Many problems in machine learning and game theory can be written in the form $\min_{x \in X} \max_{y \in Y} \mathcal{L}(x, y)$, where \mathcal{L} is a convex-concave function and X, Y are reflexive Banach spaces, e.g. regularized finite-sum loss minimization, imaging models, and sequential two-player zero-sum games [Chambolle and Pock, 2011, Kroer et al., 2018]. Even though convex duality often allows reformulating this saddle-point problem as a single convex program, first-order methods (FOMs) such as Chambolle & Pock’s Primal-Dual Algorithm (PDA, Chambolle and Pock [2011]), Mirror Descent [Nemirovski and Yudin, 1983] or Mirror Prox [Nemirovski, 2004] are typically preferred for large instances. This is due to the expensive matrix calculations involved in IPMs or the simplex algorithm. Naively, one may hope to apply FOMs directly to the robust MDP problem, which looks superficially similar to the saddle-point problem. However, since the robust MDP problem is not convex-concave FOMs may fail to converge.

Our main contributions can be summarized as follows.

A First-Order Method for Robust MDP. We present a new algorithmic framework for solving robust MDPs that is significantly more scalable than previous methods. Our algorithm adapts FOMs for solving static zero-sum games to a dynamic setting with varying payoff matrices. Only cheap proximal mappings need to be computed at each iteration. Our framework interleaves FOM updates with occasional approximate VI updates. By carefully controlling the pace of VI updates, and developing bounds on the change in the payoff matrices of the zero-sum games, we show that the ergodic *average of policies* generated by our framework converges (in value) at a rate of nearly $\frac{1}{T}$ in terms of the number of FOM steps T . Note the critical difference with the classical analysis of Value Iteration algorithms, which rely on the *last-iterate* convergence of the sequence of *vector iterates*.

Suitable Proximal Setups. Our algorithmic framework is general and works for any uncertainty set for which a suitable proximal setup exists. We instantiate our algorithm on KL and ellipsoidal uncertainty sets. To the best of our knowledge, our algorithm is the first to address s -rectangular KL uncertainty sets for robust MDPs, and is the most scalable for ellipsoidal s -rectangular uncertainty sets in terms of number of states and actions.

Empirical Performance. We focus our numerical experiments on ellipsoidal and KL uncertainty sets. We investigate several proximal setups, and find that an ℓ_2 setup performs better than an ℓ_1 setup, despite better theoretical guarantees for the ℓ_1 setup. Similar observations have been made for numerical performance on stationary saddle-point optimization [Chambolle and Pock, 2016, Gao et al., 2019]. Finally, we show that our approach is significantly more scalable than state-of-the-art VI setups, both on random instances and on applications inspired from healthcare and machine replacement.

Related work. We now present a summary of the most related literature.

Approximate value iteration and Regularized MDP. For the *nominal* MDP setting, approximate Value Iteration [de Farias and Roy, 2003, Petrik, 2010, Scherrer et al., 2015] considers inexact Bellman updates which arise from sample-based errors or function approximation; note that contrary to works involving value function approximation, we are solving the MDP up to any chosen accuracy. Geist et al. [2019] adds KL regularization to the VI update for nominal MDP and relate this to Mirror Descent. In contrast to Geist et al. [2019], we focus on robust MDPs, where VI requires computing the robust Bellman operator. Our framework is based on a connection to zero-sum games with changing payoff matrices and we use FOMs to efficiently approximate the robust Bellman update. This is very different from Geist et al. [2019], where regularized VI itself is treated as a FOM.

Faster value iteration algorithms. For nominal MDPs, several algorithms have been proposed to accelerate the convergence of VI, including Anderson mixing [Zhang et al., 2018, Geist and Scherrer, 2018] and acceleration and momentum schemes [Goyal and Grand-Clement, 2019]. However, these methods modify the VI algorithm itself, and do not accelerate the computation of each Bellman update.

Faster Bellman updates. For s, a -rectangular uncertainty sets, robust Bellman updates were studied for uncertainty sets defined by balls for the ℓ_1 and weighed ℓ_1 norms (Iyengar [2005], Ho et al. [2018]), ℓ_2 norm [Iyengar, 2005], KL-divergence [Nilim and Ghaoui, 2005] and ℓ_∞ norm [Givan et al., 1997]. To the best of our knowledge, the only paper on fast computation of robust Bellman updates for s -rectangular uncertainty sets is Ho et al. [2018] which considers weighted ℓ_1 -balls for \mathbb{P}_s and attains a complexity of $O(AS^3 \log(AS^2) \log(\epsilon^{-1}))$ for finding an ϵ -solution to the robust MDP problem. This complexity result relies on linear programming theory and cannot directly be extended to other settings for \mathbb{P}_s (e.g. ellipsoidal or KL uncertainty sets).

2 Preliminaries on Robust MDP

Notation. We write $|\mathbb{S}| = S, |\mathbb{A}| = A$ and we assume $S < +\infty, A < +\infty$. Given a policy $\mathbf{x} \in \Pi = (\Delta(A))^S$ and a kernel $\mathbf{y} \in \mathbb{P}$, we define the one-step cost vector $\mathbf{c}_{\mathbf{x}} \in \mathbb{R}^S$ and the value vector $\mathbf{v}^{\mathbf{x}, \mathbf{y}} \in \mathbb{R}^S$ as $c_{\mathbf{x}, s} = \sum_{a=1}^A x_{sa} c_{sa}, v_s^{\mathbf{x}, \mathbf{y}} = E^{\mathbf{x}, \mathbf{y}} \left[\sum_{t=0}^{\infty} \lambda^t c_{s_t a_t} \mid s_0 = s \right], \forall s \in \mathbb{S}$.

Value Iteration. We first define Value Iteration (VI) for general s -rectangular uncertainty sets. Let $\mathbb{P} = \prod_{s \in \mathbb{S}} \mathbb{P}_s$, for $\mathbb{P}_s \subseteq \mathbb{R}_+^{|\mathbb{A}| \times |\mathbb{S}|}$. and let us define the (robust) Bellman operator $F : \mathbb{R}^S \rightarrow \mathbb{R}^S$, where for $\mathbf{v} \in \mathbb{R}^S$,

$$F(\mathbf{v})_s = \min_{\mathbf{x}_s \in \Delta(A)} \max_{\mathbf{y}_s \in \mathbb{P}_s} \left\{ \sum_{a=1}^A x_{sa} (c_{sa} + \lambda \mathbf{y}_{sa}^\top \mathbf{v}) \right\}, \quad (2.1)$$

for each $s \in \mathbb{S}$. Note that with the notation $F^{\mathbf{x}, \mathbf{y}}(\mathbf{v})_s = \sum_{a=1}^A x_{sa} (c_{sa} + \lambda \cdot \mathbf{y}_{sa}^\top \mathbf{v})$, we can also write $F(\mathbf{v})_s = \min_{\mathbf{x}_s \in \Delta(A)} \max_{\mathbf{y}_s \in \mathbb{P}_s} F^{\mathbf{x}, \mathbf{y}}(\mathbf{v})_s$, which shows that the robust VI update is a stationary saddle-point problem. Solving the robust MDP problem is equivalent to computing \mathbf{v}^* , the fixed-point of F :

$$\mathbf{v}_s^* = \min_{\mathbf{x}_s \in \Delta(A)} \max_{\mathbf{y}_s \in \mathbb{P}_s} \left\{ \sum_{a=1}^A x_{sa} (c_{sa} + \lambda \cdot \mathbf{y}_{sa}^\top \mathbf{v}^*) \right\}, \forall s \in \mathbb{S}. \quad (2.2)$$

Since F is a contraction with factor λ , this can be done with the Value Iteration (VI) Algorithm:

$$\mathbf{v}_0 \in \mathbb{R}^S, \mathbf{v}_{\ell+1} = F(\mathbf{v}_\ell), \forall \ell \geq 0. \quad (\text{VI})$$

VI returns a sequence $\{\mathbf{v}_\ell\}_{\ell \geq 0}$ such that $\|\mathbf{v}^{\ell+1} - \mathbf{v}^*\|_\infty \leq \lambda \cdot \|\mathbf{v}^\ell - \mathbf{v}^*\|_\infty, \forall \ell \geq 0$. An optimal pair $(\mathbf{x}^*, \mathbf{y}^*)$ can be computed as any pair attaining the min max in $F(\mathbf{v}^*)$. An ϵ -optimal pair can be computed as a solution to (2.1), when $\|\mathbf{v} - F(\mathbf{v})\|_\infty < \epsilon(1 - \lambda)(2\lambda)^{-1}$ [Puterman, 1994]. Our algorithm relies on approximately solving 2.1 as part of VI; controlling ϵ_ℓ , the accuracy of epoch ℓ of VI, plays a crucial role in the analysis of our algorithm. In Appendix A, we present *approximate* Value Iteration, where the Bellman update $F(\mathbf{v}^\ell)$ at epoch ℓ is only computed up to accuracy ϵ_ℓ .

Ellipsoidal and KL uncertainty sets. We will show specific results for two types of s -rectangular uncertainty sets, though our algorithmic framework applies more generally, as long as appropriate proximal mappings can be computed. We consider KL s -rectangular uncertainty sets where \mathbb{P}_s equals

$$\{(\mathbf{y}_{sa})_{a \in \mathbb{A}} \in (\Delta(S))^A \mid \sum_{a \in \mathbb{A}} KL(\mathbf{y}_{sa}, \mathbf{y}_{sa}^0) \leq \alpha\}, \quad (2.3)$$

and *ellipsoidal* s -rectangular uncertainty sets where \mathbb{P}_s equals

$$\{(\mathbf{y}_{sa})_{a \in \mathbb{A}} \in (\Delta(S))^A \mid \sum_{a \in \mathbb{A}} \frac{1}{2} \|\mathbf{y}_{sa} - \mathbf{y}_{sa}^0\|_2^2 \leq \alpha\}. \quad (2.4)$$

Note that (2.4) is different from the ellipsoidal uncertainty sets considered in Ben-Tal and Nemirovski [2000], which also adds box constraints. However, Bertsimas et al. [2019] shows that the same probabilistic guarantees exist for (2.4) as in the case of the uncertainty sets considered in Ben-Tal and Nemirovski [2000]. For solving s -rectangular KL uncertainty sets, no algorithm is known (contrary to the significantly more conservative s, a -rectangular case). Wiesemann et al. [2013] solves s -rectangular ellipsoidal uncertainty sets (2.4) using conic programs; we choose to instantiate VI differently in this case as follows. Using min-max convex duality twice, we can reformulate each of the S min-max programs (2.1) into a larger convex program with linear objective and constraints, and one quadratic constraint (see (K.2) in Appendix K). Using IPMs each program can be solved up to ϵ accuracy in $O(A^{3.5} S^{3.5} \log(1/\epsilon))$ arithmetic operations (Ben-Tal and Nemirovski [2001], Section 4.6.2). Therefore, the complexity of (VI) is

$$O(A^{3.5} S^{4.5} \log^2(\epsilon^{-1})). \quad (2.5)$$

As mentioned earlier, this becomes intractable as soon as the number of states becomes on the order of hundreds, as highlighted in our numerical experiments of Section 4.

3 First-Order Methods for Robust MDPs

We start by briefly introducing first-order methods (FOMs) in the context of our problem, and giving a high-level overview of our first-order framework for solving robust MDPs. A FOM is a method that iteratively produces pairs

of solution candidates $\mathbf{x}^t, \mathbf{y}^t$, where the t 'th solution pair is derived from $\mathbf{x}^{t-1}, \mathbf{y}^{t-1}$ combined with a first-order approximation to the direction of improvement at $\mathbf{x}^{t-1}, \mathbf{y}^{t-1}$. Using only first-order information is desirable for large-scale problems because second-order information eventually becomes too slow to compute, meaning that even a single iteration of a second-order method ends up being intractable. See e.g. Beck [2017] or Ben-Tal and Nemirovski [2001] for more on FOMs.

Our algorithmic framework is based on the observation that there exists a collection of matrices $\mathbf{K}_s^* : \Delta(A) \times \mathbb{P}_s \rightarrow \mathbb{R}$, for $s \in \mathbb{S}$, such that computing an optimal solution $\mathbf{x}^*, \mathbf{y}^*$ to the robust MDP problem boils down to solving S bilinear saddle-point problems (BSPPs), each of the form

$$\min_{\mathbf{x}_s \in \Delta(A)} \max_{\mathbf{y}_s \in \mathbb{P}_s} \langle \mathbf{c}_s, \mathbf{x}_s \rangle + \langle \mathbf{K}_s^* \mathbf{x}_s, \mathbf{y}_s \rangle. \quad (3.1)$$

This is a straightforward consequence of the Bellman equation 2.1 and its reformulation using $F^{\mathbf{x}, \mathbf{y}}$. The matrix \mathbf{K}_s^* is the payoff matrix associated with the optimal value vector v^* . If we knew \mathbf{K}_s^* , then we could solve (3.1) by applying existing FOMs for solving BSPPs.

Now, obviously we do not know v^* before running our algorithm. However, we know that Value Iteration constructs a sequence $\{v_\ell\}_{\ell \geq 0}$ which converges to v^* . Letting $\{\mathbf{K}_s^\ell\}_{\ell \geq 0}$ be the associated payoff matrices for each value-vector estimate v_ℓ and state s , we thus have a sequence of payoff matrices converging to \mathbf{K}_s^* for each s . We will apply a FOM to such a sequence of BSPPs $\{\mathbf{K}_s^\ell\}_{\ell \geq 0}$ based on approximate Value Iteration updates.

Our algorithmic framework, which we call FOM-VI, works as follows. We utilize an existing primal-dual FOM for solving problems of the form (3.1), where the FOM should be of the type that generates a sequence of iterates $\mathbf{x}_t, \mathbf{y}_t$, with an ergodic convergence rate on the time-averaged iterates. Even though such FOMs are designed for a *fixed* BSPP with a single payoff matrix \mathbf{K} , we apply the FOM updates to a changing sequence of payoff matrices $\{\mathbf{K}_s^\ell\}_{\ell=1}^k$. For each payoff matrix \mathbf{K}_s^ℓ we apply T_ℓ iterations of the FOM, after which we apply an approximate VI update to generate $\mathbf{K}_s^{\ell+1}$. We refer to each step ℓ with a payoff matrix \mathbf{K}_s^ℓ as an *epoch*, while *iteration* refers to steps of our FOM. We will apply many iterations per epoch.

The convergence rate of our algorithm is, intuitively, based on the following facts: (i) the average of the iterates generated during epoch ℓ provides a good estimate of the VI update associated with v^ℓ , and (ii) the sequence of payoff matrices generated by the approximate VI updates is changing in a controlled manner, such that \mathbf{K}_s^ℓ and $\mathbf{K}_s^{\ell+1}$ are not too different.

These facts allow us to show that the averaged strategy across *all* epochs ℓ converges to a solution to (3.1) without too much degradation in the convergence rate compared to having run the same number of iterations directly on (3.1).

3.1 First-Order Method Setup

In this paper, we use the PDA algorithm of Chambolle and Pock [2016] as our FOM, but the derivations could also be performed with other FOMs whose convergence rate is based on applying a telescoping argument to a sum of descent inequalities, e.g. mirror prox of Nemirovski [2004] or saddle-point mirror descent of Ben-Tal and Nemirovski [2001]; the latter would yield a slower rate of convergence.

We now describe PDA as it applies to BSPPs such as (3.1), for an arbitrary payoff matrix \mathbf{K} and some state s . PDA relies on what we will call a *proximal setup*. A proximal setup consists of a set of norms $\|\cdot\|_X, \|\cdot\|_Y$ for the spaces of $\mathbf{x}_s, \mathbf{y}_s$, as well as *distance-generating functions* ψ_X and ψ_Y , which are 1-strongly convex with respect to $\|\cdot\|_X$ on $\Delta(A)$ and $\|\cdot\|_Y$ on \mathbb{P}_s , respectively. Using the distance-generating functions, PDA uses the *Bregman divergence*

$$D_X(\mathbf{x}, \mathbf{x}') = \psi_X(\mathbf{x}') - \psi_X(\mathbf{x}) - \langle \nabla \psi_X(\mathbf{x}), \mathbf{x}' - \mathbf{x} \rangle$$

to measure the distance between two points $\mathbf{x}, \mathbf{x}' \in \Delta(A)$. The Bregman divergence D_Y is defined analogously.

The convergence rate of PDA then depends on the maximum Bregman divergence distance $\Theta_X = \max_{\mathbf{x}, \mathbf{x}' \in \Delta(A)} D_X(\mathbf{x}, \mathbf{x}')$ between any two points, and the maximum norm $R_X = \max_{\mathbf{x} \in \Delta(A)} \|\mathbf{x}\|_X$ on $\Delta(A)$. The quantities Θ_Y and R_Y are defined analogously on \mathbb{P}_s .

Given D_X and D_Y , the associated *prox mappings* are

$$\begin{aligned} \text{prox}_{\mathbf{x}}(\mathbf{g}_x, \mathbf{x}'_s) &= \arg \min_{\mathbf{x}_s \in \Delta(A)} \langle \mathbf{g}_x, \mathbf{x} \rangle + D_X(\mathbf{x}_s, \mathbf{x}'_s), \\ \text{prox}_{\mathbf{y}}(\mathbf{g}_y, \mathbf{y}'_s) &= \arg \max_{\mathbf{y}_s \in \mathbb{P}_s} \langle \mathbf{g}_y, \mathbf{y}_s \rangle - D_Y(\mathbf{y}_s, \mathbf{y}'_s). \end{aligned}$$

Intuitively, the prox mappings generalize taking a step in the direction of the negative gradient, as in gradient descent. Given some gradient \mathbf{g}_x , $\text{prox}_x(\mathbf{g}_x, \mathbf{x}'_s)$ moves in the direction of improvement, but is penalized by the Bregman divergence $D_X(\mathbf{x}_s, \mathbf{x}'_s)$, which attempts to ensure that we stay in a region where the first-order approximation is still good.

Given step sizes $\tau, \sigma > 0$ and current iterates $\mathbf{x}_s^t, \mathbf{y}_s^t$, PDA generates the iterates for $t + 1$ by taking prox steps in the negative gradient direction given the current strategies:

$$\begin{aligned}\mathbf{x}_s^{t+1} &= \text{prox}_x(\tau \mathbf{K}^\top \mathbf{y}_s^t, \mathbf{x}_s^t), \\ \mathbf{y}_s^{t+1} &= \text{prox}_y(\sigma \mathbf{K}(2\mathbf{x}_s^{t+1} - \mathbf{x}_s^t), \mathbf{x}_s^t),\end{aligned}\tag{3.2}$$

Note that for the \mathbf{y}_s^{t+1} update, the ‘‘direction of improvement’’ is measured according to the extrapolated point $2\mathbf{x}_s^{t+1} - \mathbf{x}_s^t$, as opposed to at either \mathbf{x}_s^t or \mathbf{x}_s^{t+1} . If a simpler single current iterate is used to take the gradient for \mathbf{y}_s^{t+1} , then the overall PDA setup yields an algorithm that converges at a $O(1/\sqrt{T})$ rate. The extrapolation is used to get a stronger $O(1/T)$ rate.

Let $\Omega = 2(\Theta_X/\tau + \Theta_Y/\sigma)$ and let $\tau, \sigma > 0$ be such that, for $L_{\mathbf{K}} \geq \sup_{\|\mathbf{x}\|_X \leq 1, \|\mathbf{y}\|_Y \leq 1} \langle \mathbf{K}\mathbf{x}, \mathbf{y} \rangle$, we have

$$\left(\frac{1}{\tau} - L_f\right) \frac{1}{\sigma} \geq L_{\mathbf{K}}^2.\tag{3.3}$$

After T iterations of PDA, we can construct weighted averages $(\bar{\mathbf{x}}^T, \bar{\mathbf{y}}^T) = (1/S_T) \sum_{t=1}^T \omega_t(\mathbf{x}_t, \mathbf{y}_t)$ of all iterates, using weights $\omega_1, \dots, \omega_T$ and normalization factor $S_T = \sum_{t=1}^T \omega_t$. In the case of a static BSPP, if the stepsizes are chosen such that they satisfy (3.3), then the average of the iterates from PDA satisfies the convergence rate:

$$\max_{\mathbf{y} \in \mathbb{P}_s} \langle \mathbf{K} \bar{\mathbf{x}}^T, \mathbf{y} \rangle - \min_{\mathbf{x} \in \Delta(A)} \langle \mathbf{K} \mathbf{x}, \bar{\mathbf{y}}^T \rangle \leq \Omega \omega_T / S_T.$$

Here we are using the weighted average of iterates, as in Gao et al. [2019], see Appendix B. Since PDA applies the two prox mappings (3.2) at every iteration, it is crucial that these prox mappings can be computed efficiently. Ideally, in time roughly linear in the dimension of the iterates. A significant part of our contribution is to show that this is indeed the case for several important types of uncertainty sets.

In our setting, where the payoff matrix \mathbf{K}_s^ℓ in the BSPP is changing over time, the existing convergence rate for PDA does not apply. Instead, we have to consider how to deal with the error that is introduced in the process due to the changing payoffs.

3.2 First-Order Method Value Iteration (FOM-VI)

We now describe our algorithm in detail, as well as the choices of $\|\cdot\|_X, \|\cdot\|_Y$ that lead to tractable proximal updates (3.2). As we have described in (3.1), given a vector $\mathbf{v} \in \mathbb{R}^S$ and $s \in \mathbb{S}$, the matrix $\mathbf{K}_s \in \mathbb{R}^{A \times A \times S}$ is defined such that

$$F_s^{\mathbf{x}; \mathbf{y}}(\mathbf{v}) = \langle \mathbf{c}_s, \mathbf{x}_s \rangle + \langle \mathbf{K}_s \mathbf{x}_s, \mathbf{y}_s \rangle.$$

We will write this as $\mathbf{K} = \mathbf{K}[\mathbf{v}]$. The pseudocode for the FOM-VI algorithm is given in Algorithm 1. At each epoch ℓ , we have some current estimate v^ℓ of the value vector, which is used to construct the payoff matrix \mathbf{K}^ℓ for the ℓ 'th BSPP. For each state s , we then run T_ℓ iterations of PDA, where, crucially, the first such iteration starts from the last iterates $(\mathbf{x}_{\tau_\ell}, \mathbf{y}_{\tau_\ell})$ generated at the previous epoch. The average iterate constructed from just these T_ℓ iterations is then used to construct the next value vector $v_s^{\ell+1}$ via an approximate VI update (lines 11 and 12). Finally, after the last epoch k , we output the average of all the iterates generated across all the epochs, using the weights $\omega_1, \dots, \omega_T$.

We prove that FOM-VI satisfies the following convergence rate. We state our results for the two special cases where the norms $\|\cdot\|_X$ and $\|\cdot\|_Y$ are both equal to the ℓ_1 norm (we call this the ℓ_1 setup) or ℓ_2 norm (ℓ_2 setup) on the spaces $\Delta(A), \mathbb{P}_s$. FOM-VI could also be instantiated with other norms. The proof is in Appendix C.

Theorem 3.1. *Assume that the stepsizes τ, σ are such that (3.3) holds, and for each epoch ℓ , we set $T_\ell = \ell^q$ for some $q \in \mathbb{N}$. Let $\bar{\mathbf{x}}^T, \bar{\mathbf{y}}^T$ be the averages of the FOM-VI iterates using the weights w_1, \dots, w_T . Then for all states $s \in \mathbb{S}$,*

$$\max_{\mathbf{y} \in \mathbb{P}_s} F^{\bar{\mathbf{x}}^T; \mathbf{y}}(\mathbf{v}^*)_s - \min_{\mathbf{x} \in \Delta(A)} F^{\mathbf{x}; \bar{\mathbf{y}}^T}(\mathbf{v}^*)_s \leq O\left(C R_X R_Y \left(\frac{\Theta_X}{\tau} + \frac{\Theta_Y}{\sigma}\right) \left(\frac{\lambda^{T^{1/(q+1)}}}{T^{1/(q+1)}} + \frac{1}{T^{q/(q+1)}}\right)\right),$$

with $C = 1$ in the ℓ_1 setup, and $C = \sqrt{S}$ in the ℓ_2 setup.

Algorithm 1 First-order Method for Robust MDP with s -rectangular uncertainty set.

- 1: **Input** Number of epochs k , number of iterations per epoch T_1, \dots, T_k , weights $\omega_1, \dots, \omega_T$, and stepsizes τ, σ .
 - 2: **Initialize** $\ell = 1$, $\mathbf{v}^\ell = \mathbf{0}$, and $\mathbf{x}^0, \mathbf{y}^0$ at random.
 - 3: **for** epoch $\ell = 1, \dots, k$ **do**
 - 4: **for** $s \in \mathbb{S}$ **do**
 - 5: Set $\tau_\ell = T_1 + \dots + T_{\ell-1}$
 - 6: **for** $t = \tau_\ell, \dots, \tau_\ell + T_\ell$ **do**
 - 7: $\mathbf{x}_s^{t+1} = \text{prox}_x(\tau \mathbf{K}_s[\mathbf{v}^\ell]^\top \mathbf{y}_s^t, \mathbf{x}_s^t)$
 - 8: $\mathbf{y}_s^{t+1} = \text{prox}_y(\sigma \mathbf{K}_s[\mathbf{v}^\ell](2\mathbf{x}_s^{t+1} - \mathbf{x}_s^t), \mathbf{y}_s^t)$
 - 9: **end for**
 - 10: $S_\ell = \sum_{t=\tau_\ell}^{\tau_\ell+T_\ell} \omega_t$
 - 11: $\bar{\mathbf{x}}_s^\ell = \sum_{t=\tau_\ell}^{\tau_\ell+T_\ell} \frac{\omega_t}{S_\ell} \mathbf{x}_s^t, \bar{\mathbf{y}}_s^\ell = \sum_{t=\tau_\ell}^{\tau_\ell+T_\ell} \frac{\omega_t}{S_\ell} \mathbf{y}_s^t$
 - 12: Update $\mathbf{v}_s^{\ell+1} = F^{\bar{\mathbf{x}}_s^\ell, \bar{\mathbf{y}}_s^\ell}(\mathbf{v}^\ell)_s$.
 - 13: **end for**
 - 14: **end for**
 - 15: **Output** $\bar{\mathbf{x}}_s^T = \sum_{t=1}^T \frac{\omega_t}{S_T} \mathbf{x}_s^t, \bar{\mathbf{y}}_s^T = \sum_{t=1}^T \frac{\omega_t}{S_T} \mathbf{y}_s^t, \forall s \in \mathbb{S}$
-

3.3 Tractable proximal setups for Algorithm 1

In the previous section we saw that FOM-VI instantiated with appropriate proximal setups yields an attractive convergence rate. For a given proximal setup, the convergence rate in Theorem 3.1 depends on the maximum-norm quantities R_X, R_Y and the polytope diameter measures Θ_X, Θ_Y . However, another important issue was previously not discussed: in order to run FOM-VI we must compute the iterates $\mathbf{x}_s^{t+1}, \mathbf{y}_s^{t+1}$, which means that the updates in (3.2) must be fast to compute (ideally in closed form). We next present several tractable proximal setups for Algorithm 1.

Tractable updates for $\Delta(A)$. Since decision space for x is a simplex, we can apply well-known results to get a proximal setup. For the ℓ_2 setup (i.e. where $\|\cdot\|_X = \|\cdot\|_2$), we can set $\psi_X(\mathbf{x}) = (1/2)\|\mathbf{x}\|_2^2$, in which case D_X is the squared Euclidean distance. For this setup, $\Theta_X = 1$, and \mathbf{x}_s^{t+1} can be computed in $A \log A$ time, using a well-known algorithm based on sorting [Ben-Tal and Nemirovski, 2001].

For the ℓ_1 setup, (i.e. where $\|\cdot\|_X = \|\cdot\|_1$), we set $\psi_X(\mathbf{x}) = \text{ENT}(\mathbf{x}) \stackrel{\text{def}}{=} \sum_i x_i \log x_i$ (i.e. the negative entropy), in which case D_X is the *KL divergence*. The advantage of this setup is that the strong convexity is with respect to the ℓ_1 norm, which makes the Lipschitz associated to the payoff matrix a constant (as opposed to \sqrt{S} for the ℓ_2 norm), while the polytope diameter is only $\Theta_X = \log A$. Finally, \mathbf{x}_s^{t+1} can be computed in closed form. Thus, from a theoretical perspective, the ℓ_1 setup is more attractive than the ℓ_2 setup for $\Delta(A)$. This is well-known in the literature.

In all cases, $R_X = 1$, since \mathbf{x} comes from a simplex.

Tractable updates for ellipsoidal uncertainty. The proximal updates for y turn out to be more complicated. In the first place, they depend heavily on the form of \mathbb{P}_s . First, we present our results for the case where \mathbb{P}_s is an ellipsoidal s -rectangular uncertainty set as in (2.4). We present both ℓ_1 and ℓ_2 setups.

In the ℓ_2 setup for ellipsoidal uncertainty, we let $\|\cdot\|_Y$ be the ℓ_2 norm, and $\psi_Y(\mathbf{y}) = (1/2)\|\mathbf{y}\|_2^2$. The Bregman divergence $D_Y(\mathbf{y}, \mathbf{y}')$ is then simply the squared Euclidean distance. In this case, we get that $R_Y = \sqrt{A}$, since the squared norm of each individual simplex is at most one, and then we take the square root. The polytope diameter is $\Theta_Y = 2A$ for the same reason. We show in Proposition 3.2 below that the iterate \mathbf{y}_s^{t+1} can be computed efficiently.

In the ℓ_1 setup for ellipsoidal uncertainty, we let $\|\cdot\|_Y$ be the ℓ_1 norm, and $\psi_Y(\mathbf{y}) = (A/2) \sum_{a=1}^A \text{ENT}(\mathbf{y}_a)$, where $\text{ENT}(\mathbf{y}_a)$ is the negative entropy function. The Bregman divergence $D_Y(\mathbf{y}, \mathbf{y}') = (A/2) \sum_{a=1}^A \text{KL}(\mathbf{y}_a, \mathbf{y}'_a)$ is then a sum over KL divergences on each action. In this case, we get that $R_Y = A$, since we are taking the ℓ_1 norm over A simplexes, while the polytope diameter is $\Theta_Y = A^2 \log S$.

Proposition 3.2 shows that for both our ℓ_2 -based and ℓ_1 -based setup for y , the next iterate can be computed efficiently. We present a detailed proof in Appendix D.

Proposition 3.2. *For the ℓ_2 setup, the proximal update (3.2) with uncertainty set (2.4) can be approximated up to ϵ in a number of arithmetic operations of $O(AS \log(S) \log(\epsilon^{-1}))$.*

For the ℓ_1 setup, the proximal update (3.2) with uncertainty set (2.4) can be approximated up to ϵ in a number of arithmetic operations of $O(AS \log^2(\epsilon^{-1}))$.

Tractable updates for KL uncertainty. As in the case of ellipsoidal uncertainty, we present both ℓ_1 and ℓ_2 setups for KL uncertainty. The setups are exactly the same as for ellipsoidal uncertainty (i.e. same norms, distance functions, and Bregman divergences), and all constants remain the same. The reason that all constants remain the same is because our bounds on the maximum norms and Θ_Y , for both uncertainty set types, are based on bounding these values over the bigger set consisting of the Cartesian product of A simplexes. The question thus becomes whether (3.2) can be computed efficiently (for y) when D_Y is the sum over KL divergences on each action. We present our results in the following proposition; a detailed proof can be found in Appendix F.

Proposition 3.3. *For the ℓ_2 setup, the proximal update (3.2) with uncertainty set (2.3) can be approximated up to ϵ in a number of arithmetic operations in $O(AS \log^2(\epsilon^{-1}))$.*

For the ℓ_1 setup, the proximal update (3.2) with uncertainty set (2.3) can be approximated up to ϵ in a number of arithmetic operations in $O(AS \log(\epsilon^{-1}))$.

Remark 3.4. At a cursory reading, our results in Propositions 3.2 and 3.3 may seem similar to those of Nilim and Ghaoui [2005] and Iyengar [2005]. Both authors introduce bisection algorithms for computing Bellman updates, but these are for the simpler case of (s, a) -rectangular uncertainty sets. In that case, the Bellman updates can be computed by enumerating the set of actions $a \in \mathbb{A}$, since an optimal solution exists among the set of pure actions. In contrast, in our setting the optimal $x \in \Delta(A)$ may require randomization, which is why we must solve a min-max problem as in (2.1).

3.4 Complexity of Algorithm 1

Armed with our various proximal setups, we can finally state the performance guarantees provided by FOM-VI explicitly for the various setups. Since the constants for the ℓ_1 and ℓ_2 setups are the same for both KL and ellipsoidal uncertainty sets, we start by stating a single theorem which gives a bound on the error after T iterations for either type of uncertainty set. The following theorem works for any polynomial scheme for choosing the iterate weights when averaging, as well as how many FOM iterations to perform in-between each VI update. Details are given in Appendix E.

Theorem 3.5. *Let $p, q \in \mathbb{N}$ and at time step $t \geq 0$, let the iterate weight be $\omega_t = t^p$, and the number of FOM iterations at epoch ℓ be $T_\ell = \ell^q$. After T iterations of Algorithm 1, $\max_{\mathbf{y} \in \mathbb{P}_s} F^{\bar{\mathbf{x}}^T, \mathbf{y}}(\mathbf{v}^*)_s - \min_{\mathbf{x} \in \Delta(A)} F^{\mathbf{x}, \bar{\mathbf{y}}^T}(\mathbf{v}^*)_s$ is upper bounded by*

$$\begin{aligned} & \bullet O\left(A^2 \sqrt{\frac{\log(S)}{\log(A)}} \left(\frac{1}{T^{q/(q+1)}} + \frac{\lambda^{T^{1/(q+1)}}}{T^{1/(q+1)}}\right)\right) \text{ in the } \ell_1 \text{ setup,} \\ & \bullet O\left(AS \left(\frac{1}{T^{q/(q+1)}} + \frac{\lambda^{T^{1/(q+1)}}}{T^{1/(q+1)}}\right)\right) \text{ in the } \ell_2 \text{ setup.} \end{aligned}$$

The careful reader may notice that the choice of $p \in \mathbb{N}$ in our polynomial averaging scheme does not figure in the bound of Theorem 3.5: any valid choice of p leads to the same bound. However, in practice the choice of p turns out to be very important as we shall see later. Secondly, the reader may notice an interesting dependence on q : the term $O(1/T^{q/(q+1)})$ gets better as q increases; while larger q worsens the exponential rate with base λ in the term $O(\lambda^{T^{1/(q+1)}}/T^{1/(q+1)})$. For any fixed q , the dominant term is $O(1/T^{q/(q+1)})$.

Complexity for ellipsoidal uncertainty sets. We will now combine Proposition 3.2, which gives the cost per iteration of FOM-VI, with Theorem 3.5, to get a total complexity of FOM-VI when considering both the number of iterations and cost per iteration.

First, let us consider $q = 2$, which is the setup we will focus on in our experiments. The complexity of the ℓ_1 setup is $O\left(A^4 S^2 \left(\frac{\log(S)}{\log(A)}\right)^{0.75} \log^2(\epsilon^{-1}) \epsilon^{-1.5}\right)$ and for the ℓ_2 setup it is $O\left(A^{2.5} S^{3.5} \log(S) \log(\epsilon^{-1}) \epsilon^{-1.5}\right)$. These results are better than the complexity of VI in terms of the number of states and actions. This comes at the cost of the dependence on the desired accuracy ϵ , which is worse than for VI. This is of course expected when applying a first-order method rather than IPMs. However, in practice we expect that our algorithms will be preferable when solving problems with large A and S , as is often the case with first-order methods. Indeed, we find numerically that this occurs for $S, A \geq 50$ on ellipsoidal uncertainty sets (see Section 4).

Next, let us consider what happens as q gets large. In that case, the complexity of the ℓ_1 setup approaches $O\left(A^3 S^2 (\log(S)/\log(A))^{0.5} \log^2(\epsilon^{-1}) \epsilon^{-1}\right)$, while the complexity of the ℓ_2 setup approaches

$O(A^2 S^3 \log(S) \log(\epsilon^{-1}) \epsilon^{-1})$. This last complexity result is $O(A^{1.5} S^{1.5})$ better than the VI complexity (2.5) in terms of instance size.

Next let us compare the ℓ_1 and ℓ_2 setups. When $S = A$, the ℓ_2 and ℓ_1 setup have better dependence on number of states and actions than VI (by 2 order of magnitudes). If the number of actions A is considered a constant, then the ℓ_1 has better convergence guarantees than the ℓ_2 setup. However, each proximal update in the ℓ_1 setup requires two interwoven binary searches over Lagrange multipliers, which can prove time-consuming in practice, as we show in our numerical experiments.

Complexity for KL uncertainty sets. Similarly to ellipsoidal uncertainty sets, we can analyze our performance on KL uncertainty sets. Again we combine Proposition 3.3 with Theorem 3.5. For $q = 2$, the ℓ_1 setup has complexity $O\left(A^4 S^2 \left(\frac{\log(S)}{\log(A)}\right)^{0.75} \log(\epsilon^{-1}) \epsilon^{-1.5}\right)$ for returning an ϵ -optimal solution, while the ℓ_2 setup has complexity

$O(A^{2.5} S^{3.5} \log(\epsilon^{-1}) \epsilon^{-1.5})$. For large q , the complexity approaches $O\left(A^3 S^2 \left(\frac{\log(S)}{\log(A)}\right)^{0.5} \log(\epsilon^{-1}) \epsilon^{-1}\right)$ for the ℓ_1 setup and $O(A^2 S^3 \log(\epsilon^{-1}) \epsilon^{-1})$ for the ℓ_2 setup. To the best of our knowledge, this is the first algorithmic result for s -rectangular KL uncertainty sets.

Finally, note that in terms of storage complexity, all our setups only need to store the current value vector $\mathbf{v}^\ell \in \mathbb{R}^S$ and the running weighted average $(\bar{\mathbf{x}}^\ell, \bar{\mathbf{y}}^\ell)$ of the iterates. In total, we need to store $O(S^2 A)$ coefficients, which is the same as the number of decision variables of a solution.

4 Numerical experiments

In this section we study the performance of our approach numerically. We focus here on ellipsoidal uncertainty sets, where we can compare our methods to Value Iteration. We present results for KL uncertainty sets in Appendix L.

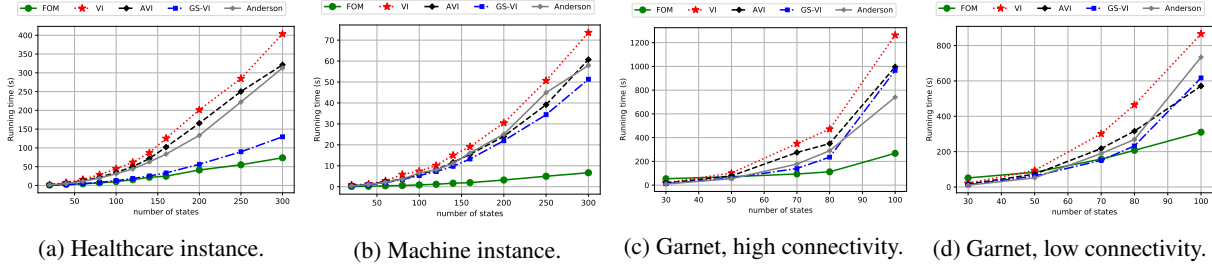


Figure 1: Comparison of FOM-VI with variants of Value Iteration on four MDP domains.

Duality gap in the robust MDP problem. For a given policy-kernel pair (\mathbf{x}, \mathbf{y}) , we measure the performance as the duality gap $(\text{DG}) = \max_{\mathbf{y}' \in \mathbb{P}} R(\mathbf{x}, \mathbf{y}') - \min_{\mathbf{x}' \in \Pi} R(\mathbf{x}', \mathbf{y})$. Note that $(\text{DG}) \leq \epsilon$ implies that \mathbf{x} is 2ϵ -optimal in the robust MDP problem.

Best empirical setup of Algorithm 1. For the sake of conciseness, our extensive comparisons of the various proximal setups and parameter choices $(p, q \in \mathbb{N})$ are presented in Appendix H. Here we focus on the conclusions. The proximal setup with the best empirical performance is the ℓ_2 setup where $(\|\cdot\|_X, \|\cdot\|_Y) = (\ell_2, \ell_2)$, even though its theoretical guarantees may be worse than the ℓ_1 setup (for large state space); this is similar to the matrix-game setting [Gao et al., 2019]. For averaging the PD iterates, an increasing weight scheme, i.e. $p \geq 1$ in $\omega_t = t^p$, is clearly stronger (this is again similar to the matrix-game setting). We also recommend setting $q = 2$ (or even larger), as this leads to better empirical performance for the true duality gap (DG) in the settings where we could compute that duality gap.

4.1 Comparison with Value Iteration

We present our comparisons with the VI algorithm in Figures 1a-1d. We also compare FOM-VI with Gauss-Seidel VI (*GS-VI*, Puterman [1994]), Anderson VI (*Anderson*, Geist and Scherrer [2018]), and *Accelerated VI* (*AVI*, Goyal and Grand-Clement [2019]), see Appendix K. The y-axis shows the number of seconds it takes each algorithm to compute

an ϵ -optimal policy, for $\epsilon = 0.1$. Following our analysis of the various setups for our algorithm, these plots focus on the ℓ_2 setup with $(p, q) = (2, 2)$.

Empirical setup. All the simulations are implemented in Python 3.7.3, and were performed on a laptop with 2.2 GHz Intel Core i7 and 8 GB of RAM. We use Gurobi 8.1.1 to solve any linear or quadratic optimization problems involved. In order to obtain an ϵ -solution of the robust MDP problem with the value iteration algorithms, we use the stopping condition $\|\mathbf{v}_{s+1} - \mathbf{v}_s\|_\infty \leq \epsilon \cdot (1 - \lambda) \cdot (2\lambda)^{-1}$ (Chapter 6.3 in Puterman [1994]). We stop Algorithm 1 as soon as $(DG) \leq \epsilon/2$. We initialize the algorithms with $\mathbf{v}_0 = \mathbf{0}$. At epoch ℓ of VI AVI and Anderson, we warm-start each computation of $F(\mathbf{v}^\ell)$ with the optimal solution obtained from the previous epoch $\ell - 1$.

We consider two type of instances for our simulation. The first type of instances is inspired from real-life application and consists of a healthcare management instance and a machine replacement instance. The second type is based on random *Garnet* MDPs, a class of random MDP instances widely used for benchmarking algorithms.

Results for healthcare instances. We consider an MDP instance inspired from a healthcare application. We model the evolution of a patient’s health using a Markov chain, using a simplification of the models used in Goh et al. [2018], Grand-Clement et al. [2020]. Note that such a model is prone to errors as (i) the Markovian assumption is only an approximation of the true dynamics of the patient’s health, (ii) the presence of unobservable confounders may introduce biases in our observed transitions. Therefore, it is important to account for model misspecification in this setting. More specifically, we consider an MDP where there are $S - 1$ health states, one ‘mortality’ state and three actions (drug level), corresponding to high, medium and low drug levels. The state 1 corresponds to a healthy condition while the state $S - 1$ is more likely to lead to mortality. The goal of the decision maker is to prescribe a given drug dosage (low/high/medium) at every state, in order to keep the patient alive (avoiding the mortality state), while minimizing the invasiveness of the treatment. We observe $N = 60$ samples around the nominal kernel transitions, presented in Figures 5a-5c in the appendices, and we construct ellipsoidal uncertainty sets with radius $\alpha = \sqrt{SA}$. Figure 1a shows the results, where our algorithm outperforms VI by about one order of magnitude on this structured and simple MDP instance, even though GS-VI performs well better than VI too. Additionally, our algorithm scales much better with instance size.

Results for Machine Replacement Problems We also consider a machine replacement problem studied by Delage and Mannor [2010] and Wiesemann et al. [2013]. The problem is to design a replacement policy for a line of machines. The states of the MDP represent age phases of the machine and the actions represent different repair or replacement options. Even though the transition parameters can be estimated from historical data, one often does not have access to enough historical data to exactly assess the probability of a machine breaking down when in a given condition. Additionally, the historical data may contain errors; this warrants the use of a robust model for finding a good replacement policy. In particular, the machine replacement problem involves a machine whose set of possible conditions are described by S states. There are two actions: *repair* and *no repair*. The first $S - 2$ states are operative states. The states 1 to $S - 2$ model the condition of the machine, with 1 being perfect condition and $S - 2$ being worst condition. There is a cost of 0 for states 1, ..., $S - 3$; letting the machine reach the worst operative state $S - 2$ is penalized with a cost of 20. The last two states $S - 1$ and S are states representing when the machine is being repaired. The state $S - 1$ is a standard repair state and has a cost of 2, while the last state S is a longer and more costly repair state and has cost 10. The initial distribution is uniform across states. Figures describing the MDP can be found in Appendix J. On this instance, FOM-VI clearly outperforms every variants of VI, as seen on Figure 1b.

Random Garnet MDP instances. We generate Garnet MDPs (Generalized Average Reward Non-stationary Environment Test-bench, Archibald et al. [1995], Bhatnagar et al. [2007]), which are an abstract class of MDPs parametrized by a branching factor n_{branch} , equal to the proportion of reachable next states from each state-action pair (s, a) . Garnet MDPs are a popular class of finite MDPs used for benchmarking algorithms for MDPs [Tarbouriech and Lazaric, 2019, Piot et al., 2016, Jian et al., 2019]. The parameter n_{branch} controls the level of connectivity of the underlying Markov chains. We test our algorithm for high connectivity ($n_{branch} = 50\%$, Figure 1c) and low connectivity ($n_{branch} = 20\%$, Figure 1d) in our simulations. We draw the cost parameters at random uniformly in $[0, 10]$ and we fix a discount factor $\lambda = 0.8$. The radius α of the ℓ_2 ball from the uncertainty set (2.4) is set to $\alpha = \sqrt{n_{branch} \times A}$.

In Figures 1c-1d, we note that for smaller instances, the performance of FOM-VI is similar to both VI, AVI, GS-VI and Anderson. This is expected: our algorithm has worse convergence guarantees in terms of the dependence in ϵ , but better guarantees in terms of the number of state-actions S, A . When the number of states and actions grows larger, FOM-VI performs significantly better than the three other methods.

References

- TW Archibald, KIM McKinnon, and LC Thomas. On the generation of Markov decision processes. *Journal of the Operational Research Society*, 46(3):354–361, 1995.
- Amir Beck. *First-order methods in optimization*. SIAM, 2017.
- Aharon Ben-Tal and Arkadi Nemirovski. Robust solutions of linear programming problems contaminated with uncertain data. *Mathematical programming*, 88(3):411–424, 2000.
- Aharon Ben-Tal and Arkadi Nemirovski. *Lectures on modern convex optimization: analysis, algorithms, and engineering applications*, volume 2. Siam, 2001.
- Dimitri Bertsekas. *Dynamic Programming and Optimal Control*, volume 2. Athena Scientific, 2007.
- Dimitris Bertsimas, Dick den Hertog, and Jean Pauphilet. Probabilistic guarantees in robust optimization. 2019.
- Shalabh Bhatnagar, Richard S Sutton, Mohammad Ghavamzadeh, and Mark Lee. Naturalgradient actor-critic algorithms. *Automatica*, 2007.
- Antonin Chambolle and Thomas Pock. A first-order primal-dual algorithm for convex problems with applications to imaging. *Journal of mathematical imaging and vision*, 40(1):120–145, 2011.
- Antonin Chambolle and Thomas Pock. On the ergodic convergence rates of a first-order primal–dual algorithm. *Mathematical Programming*, 159(1-2):253–287, 2016.
- Patrick L Combettes and Jean-Christophe Pesquet. Proximal splitting methods in signal processing. In *Fixed-point algorithms for inverse problems in science and engineering*, pages 185–212. Springer, 2011.
- D. de Fariás and B. Van Roy. The linear programming approach to approximate dynamic programming. *Operations research*, 51(6):850–865, 2003.
- E. Delage and S. Mannor. Percentile optimization for markov decision processes with parameter uncertainty. *Operations Research*, 58(1):203 – 213, 2010.
- John Duchi, Shai Shalev-Shwartz, Yoram Singer, and Tushar Chandra. Efficient projections onto the L-1 ball for learning in high dimensions. In *Proceedings of the 25th international conference on Machine learning*, pages 272–279, 2008.
- Victor Gabillon, Mohammad Ghavamzadeh, and Bruno Scherrer. Approximate dynamic programming finally performs well in the game of Tetris. In *Advances in neural information processing systems*, pages 1754–1762, 2013.
- Yuan Gao, Christian Kroer, and Donald Goldfarb. Increasing iterate averaging for solving saddle-point problems. *arXiv preprint arXiv:1903.10646*, 2019.
- Matthieu Geist and Bruno Scherrer. Anderson acceleration for reinforcement learning. *arXiv preprint arXiv:1809.09501*, 2018.
- Matthieu Geist, Bruno Scherrer, and Olivier Pietquin. A theory of regularized Markov decision processes. *arXiv preprint arXiv:1901.11275*, 2019.
- Robert Givan, Sonia Leach, and Thomas Dean. Bounded parameter Markov decision processes. In *European Conference on Planning*, pages 234–246. Springer, 1997.
- Joel Goh, Mohsen Bayati, Stefanos A Zenios, Sundeep Singh, and David Moore. Data uncertainty in Markov chains: Application to cost-effectiveness analyses of medical innovations. *Operations Research*, 66(3):697–715, 2018.
- Vineet Goyal and Julien Grand-Clement. Robust Markov decision process: Beyond rectangularity. *arXiv preprint arXiv:1811.00215*, 2018.
- Vineet Goyal and Julien Grand-Clement. A first-order approach to accelerated value iteration. *arXiv preprint arXiv:1905.09963*, 2019.
- Julien Grand-Clement, Carri W Chan, Vineet Goyal, and Gabriel Escobar. Robust policies for proactive ICU transfers. *arXiv preprint arXiv:2002.06247*, 2020.

- C.P. Ho, M. Petrik, and W. Wiesemann. Fast Bellman updates for Robust MDPs. *Proceedings of the 35th International Conference on Machine Learning (ICML), Stockholm*, 2018.
- Zhaolin Hu and L Jeff Hong. Kullback-leibler divergence constrained distributionally robust optimization. *Available at Optimization Online*, 2013.
- G. Iyengar. Robust dynamic programming. *Mathematics of Operations Research*, 30(2):257–280, 2005.
- QIAN Jian, Ronan Fruit, Matteo Pirota, and Alessandro Lazaric. Exploration bonus for regret minimization in discrete and continuous average reward mdps. In *Advances in Neural Information Processing Systems*, pages 4890–4899, 2019.
- Anatoli Juditsky, Arkadi Nemirovski, et al. First order methods for nonsmooth convex large-scale optimization. *Optimization for Machine Learning*, 2011.
- Christian Kroer, Kevin Waugh, Fatma Kılınc-Karzan, and Tuomas Sandholm. Faster algorithms for extensive-form game solving via improved smoothing functions. *Mathematical Programming*, pages 1–33, 2018.
- Miguel Sousa Lobo, Lieven Vandenbergh, Stephen Boyd, and Hervé Lebret. Applications of second-order cone programming. *Linear algebra and its applications*, 284(1-3):193–228, 1998.
- Arkadi Nemirovski. Prox-method with rate of convergence $O(1/t)$ for variational inequalities with lipschitz continuous monotone operators and smooth convex-concave saddle point problems. *SIAM Journal on Optimization*, 15(1): 229–251, 2004.
- Arkadi Nemirovski and David Yudin. *Problem complexity and method efficiency in optimization*. 1983.
- Yurii Nesterov. A method for solving the convex programming problem with convergence rate $O(1/k^2)$. In *Dokl. akad. nauk Sssr*, volume 269, pages 543–547, 1983.
- Yurii Nesterov. *Introductory lectures on convex optimization: A basic course*, volume 87. Springer Science & Business Media, 2013.
- A. Nilim and L. El Ghaoui. Robust control of Markov decision processes with uncertain transition probabilities. *Operations Research*, 53(5):780–798, 2005.
- Marek Petrik. Optimization-based approximate dynamic programming. 2010.
- Bilal Piot, Matthieu Geist, and Olivier Pietquin. Difference of convex functions programming applied to control with expert data. *arXiv preprint arXiv:1606.01128*, 2016.
- M.L. Puterman. *Markov Decision Processes : Discrete Stochastic Dynamic Programming*. John Wiley and Sons, 1994.
- Bruno Scherrer, Mohammad Ghavamzadeh, Victor Gabillon, Boris Lesner, and Matthieu Geist. Approximate modified policy iteration and its application to the game of Tetris. *Journal of Machine Learning Research*, 16(49):1629–1676, 2015.
- Lauren N Steimle and Brian T Denton. Markov decision processes for screening and treatment of chronic diseases. In *Markov Decision Processes in Practice*, pages 189–222. Springer, 2017.
- Lauren N Steimle, David L Kaufman, and Brian T Denton. Multi-model Markov decision processes. *Optimization Online* URL http://www.optimization-online.org/DB_FILE/2018/01/6434.pdf, 2018.
- Jean Tarbouriech and Alessandro Lazaric. Active exploration in markov decision processes. *arXiv preprint arXiv:1902.11199*, 2019.
- W. Wiesemann, D. Kuhn, and B. Rustem. Robust Markov decision processes. *Operations Research*, 38(1):153–183, 2013.
- Junzi Zhang, Brendan O’Donoghue, and Stephen Boyd. Globally convergent type-I Anderson acceleration for non-smooth fixed-point iterations. *arXiv preprint arXiv:1808.03971*, 2018.

A Proofs of Section 2

A.1 Some useful lemmas

The next lemmas give bounds on some sums that appear in the proof of Proposition C.1.

Lemma A.1. *Let $\lambda \in (0, 1)$ and $k, n \in \mathbb{N}$. Then*

$$\sum_{\ell=1}^k \lambda^\ell \ell^n \leq O\left(\frac{k^n \lambda^k}{(1-\lambda)^{n+1}}\right).$$

Proof of Lemma A.1. Let us define $f : x \mapsto \frac{1-x^k}{1-x} = \sum_{\ell=1}^k x^\ell$. Then $f^{(n)}(x) = \sum_{\ell=1}^k x^\ell \ell(\ell-1)\dots(\ell-n+1)$, and

$$\sum_{\ell=1}^k \lambda^\ell \ell^n = O\left(\sum_{\ell=1}^k x^\ell \ell(\ell-1)\dots(\ell-n+1)\right).$$

We can conclude by computing the n -th derivative of f as the n -th derivative of $x \mapsto \frac{1-x^k}{1-x}$. □

Lemma A.2. *Let $\lambda \in (0, 1)$ and $q \geq 0$. Then there exists a constant $M_{\lambda,q}$ such that*

$$\sum_{t=1}^{\ell} \frac{1}{t^q \lambda^t} \leq M_{\lambda,q} \frac{1}{\ell^q \lambda^\ell}.$$

Proof of Lemma A.2. Let $\lambda^+ = \frac{1+\lambda}{2}$. Note that we always have $\lambda < \lambda^+ < 1$. For $x = 1/\lambda$, we have $x > x^+ = 1/\lambda^+ > 1$. For $f_\ell(x) = \sum_{t=1}^{\ell} \frac{x^t}{t^q}$, we have

$$f'_\ell(x) = \sum_{t=1}^{\ell} \frac{x^{t-1}}{t^{q-1}} \leq \ell^{1-q} \sum_{t=1}^{\ell} x^{t-1} \leq \ell^{1-q} \frac{x^\ell - 1}{x - 1}.$$

This proves that

$$f_\ell(x) - f_\ell(x^+) = \ell^{1-q} \int_{u=x^+}^x \frac{u^\ell - 1}{u - 1} du \leq \ell^{1-q} \frac{1}{x^+ - 1} \int_{u=x^+}^x (u^\ell - 1) du \leq \ell^{1-q} \frac{1}{x^+ - 1} \frac{1}{\ell + 1} [u^{\ell+1} - u]_{x^+}^x,$$

and finally that

$$f_\ell(x) = f_\ell(x^+) + \ell^{1-q} \frac{1}{x^+ - 1} \frac{1}{\ell + 1} (x^{\ell+1} - x - x^{+\ell+1} + x^+). \quad (\text{A.1})$$

We will prove that the right-hand side of (A.1) is itself a $O\left(\frac{x^\ell}{\ell^q}\right)$ as $\ell \rightarrow +\infty$. The proof relies on the fact that $x > x^+$,

and therefore that $\left(\frac{x^+}{x}\right)^\ell \ell^m = o(1)$, for any $m \geq 0$.

First, since $x^+ < x$, we note that

$$\frac{\ell^q}{x^\ell} \left(\ell^{1-q} \frac{1}{x^+ - 1} \frac{1}{\ell + 1} (x^{\ell+1} - x - x^{+\ell+1} + x^+) \right) = \frac{1}{x^+ - 1} \frac{\ell}{\ell + 1} \left(x - \frac{x}{x^\ell} - x^+ \left(\frac{x^+}{x}\right)^\ell + \frac{x^+}{x^\ell} \right) = O(1).$$

Now for $\frac{\ell^q}{x^\ell} f_\ell(x^+)$ we need to distinguish between the potential values of $q \in \mathbb{R}_+$.

Proof for $q = 0$.

$$\frac{\ell^q}{x^\ell} f_\ell(x^+) = \frac{1}{x^\ell} \sum_{t=1}^{\ell} x^{+t} = O\left(\frac{x^{+\ell}}{x^\ell}\right) = o(1).$$

Proof for $q \in (0, 1)$.

$$\frac{\ell^q}{x^\ell} f_\ell(x^+) = \frac{\ell^q}{x^\ell} \sum_{t=1}^{\ell} \frac{x^{+t}}{t^q} \leq \frac{\ell^q}{x^\ell} \sum_{t=1}^{\ell} x^{+t} \leq O\left(\frac{\ell x^{+\ell}}{x^\ell}\right) = o(1).$$

Proof for $q = 1$.

$$\frac{\ell^q}{x^\ell} f_\ell(x^+) = \frac{\ell}{x^\ell} \sum_{t=1}^{\ell} \frac{x^{+t}}{t} \leq \frac{\ell}{x^\ell} x^{+\ell} \log(\ell) = o(1).$$

Proof for $q \geq 1$.

$$\frac{\ell^q}{x^\ell} f_\ell(x^+) = \frac{\ell^q}{x^\ell} \sum_{t=1}^{\ell} \frac{x^{+t}}{t^q} \leq \frac{\ell^q}{x^\ell} x^{+\ell} \sum_{t=1}^{\ell} \frac{1}{t^q} \leq O\left(\frac{\ell^q x^{+\ell}}{x^\ell}\right) = o(1).$$

□

A.2 Approximate Value Iteration

We present a variant of Value Iteration where each sub-problem $F(\mathbf{v})_s$ is solved approximately.

Proposition A.3. *Suppose that for every VI epoch $\ell \geq 1$, we solve the min-max problem (2.1) up to precision $\epsilon_\ell > 0$, i.e. we compute $(\mathbf{x}^\ell, \mathbf{y}^\ell)$ such that*

$$\mathbf{v}^{\ell+1} = F^{\mathbf{x}^\ell, \mathbf{y}^\ell}(\mathbf{v}^\ell), \|\mathbf{v}^{\ell+1} - F(\mathbf{v}^\ell)\|_\infty \leq \epsilon_\ell.$$

Then we have, for any $\ell \geq 1$,

$$\begin{aligned} \|\mathbf{v}^{\ell+1} - \mathbf{v}^*\|_\infty &\leq \lambda \|\mathbf{v}^\ell - \mathbf{v}^*\|_\infty + \epsilon_\ell, \\ \|\mathbf{v}^{\ell+1} - \mathbf{v}^\ell\|_\infty &\leq \lambda \|\mathbf{v}^\ell - \mathbf{v}^{\ell-1}\|_\infty + \epsilon_\ell + \epsilon_{\ell-1}. \end{aligned}$$

In particular, this implies

$$\begin{aligned} \|\mathbf{v}^\ell - \mathbf{v}^*\|_\infty &\leq \lambda^\ell \left(\|\mathbf{v}^* - \mathbf{v}^0\|_\infty + \sum_{t=0}^{\ell-1} \frac{\epsilon_t}{\lambda^t} \right), \\ \|\mathbf{v}^{\ell+1} - \mathbf{v}^\ell\|_\infty &\leq \lambda^\ell \left(\|\mathbf{v}^1 - \mathbf{v}^0\|_\infty + \sum_{t=0}^{\ell} \frac{\epsilon_t + \epsilon_{t-1}}{\lambda^t} \right). \end{aligned}$$

Proof of Proposition A.3. We have

$$\begin{aligned} \|\mathbf{v}^* - \mathbf{v}^{t+1}\|_\infty &= \|F(\mathbf{v}^*) - \mathbf{v}^{t+1}\|_\infty \\ &= \|F(\mathbf{v}^*) - F(\mathbf{v}^t) + F(\mathbf{v}^t) - \mathbf{v}^{t+1}\|_\infty \\ &\leq \|F(\mathbf{v}^*) - F(\mathbf{v}^t)\|_\infty + \|F(\mathbf{v}^t) - \mathbf{v}^{t+1}\|_\infty \\ &\leq \lambda \|\mathbf{v}^* - \mathbf{v}^t\|_\infty + \|F(\mathbf{v}^t) - \mathbf{v}^{t+1}\|_\infty \\ &\leq \lambda \|\mathbf{v}^* - \mathbf{v}^t\|_\infty + \epsilon_t. \end{aligned}$$

Similarly,

$$\begin{aligned} \|\mathbf{v}^{\ell+1} - \mathbf{v}^\ell\|_\infty &\leq \|\mathbf{v}^{\ell+1} - F(\mathbf{v}^\ell) + F(\mathbf{v}^\ell) - \mathbf{v}^\ell\|_\infty \\ &\leq \|\mathbf{v}^{\ell+1} - F(\mathbf{v}^\ell)\|_\infty + \|F(\mathbf{v}^\ell) - \mathbf{v}^\ell\|_\infty \\ &\leq \epsilon_\ell + \|F(\mathbf{v}^\ell) - \mathbf{v}^\ell\|_\infty \\ &\leq \epsilon_\ell + \|F(\mathbf{v}^\ell) - F(\mathbf{v}^{\ell-1})\|_\infty + \|F(\mathbf{v}^{\ell-1}) - \mathbf{v}^\ell\|_\infty \\ &\leq \epsilon_\ell + \lambda \|\mathbf{v}^\ell - \mathbf{v}^{\ell-1}\|_\infty + \|F(\mathbf{v}^{\ell-1}) - \mathbf{v}^\ell\|_\infty \\ &\leq \epsilon_\ell + \lambda \|\mathbf{v}^\ell - \mathbf{v}^{\ell-1}\|_\infty + \epsilon_{\ell-1}. \end{aligned}$$

The rest of the lemma follows directly from iterating the recursions on $\|\mathbf{v}^* - \mathbf{v}^{t+1}\|_\infty$ and on $\|\mathbf{v}^{\ell+1} - \mathbf{v}^\ell\|_\infty$. □

Note that this analysis is classical and is close to the case of approximate policy iteration for non-robust MDPs [Gabillon et al., 2013, Scherrer et al., 2015]. While we treat the term ϵ_ℓ as a (chosen) error term in our algorithm, we would like to note that we can think of the term ϵ_ℓ as some random noise, coming from either function approximations or sample-based estimations (see Section 4 in Scherrer et al. [2015]).

B Details on Primal-Dual Algorithm

In this section and the following one, we use the notation $\mathcal{L}^{\mathbf{K}} : X \times Y \rightarrow \mathbb{R}$ for the operator such that

$$\mathcal{L}^{\mathbf{K}}(\mathbf{x}, \mathbf{y}) = \langle \mathbf{x}, \mathbf{c}_s \rangle + \lambda \langle \mathbf{K} \mathbf{x}, \mathbf{y} \rangle.$$

In particular, this implies that, if $\mathbf{v} \in \mathbb{R}^S$ is such that $\langle \mathbf{K} \mathbf{x}, \mathbf{y} \rangle = \sum_{a \in \mathbb{A}} x_{sa} \mathbf{y}_{sa}^\top \mathbf{v}$, we have

$$\mathcal{L}^{\mathbf{K}}(\mathbf{x}, \mathbf{y}) = \sum_{a \in \mathbb{A}} x_{sa} (c_{sa} + \lambda \mathbf{y}_{sa}^\top \mathbf{v}) = F_s^{\mathbf{x}, \mathbf{y}}(\mathbf{v}). \quad (\text{B.1})$$

We present more details about the convergence rate of PDA. In particular, we have the following proposition [Chambolle and Pock, 2016, Gao et al., 2019].

Proposition B.1 (Chambolle and Pock [2016], Gao et al. [2019]). *For $(\mathbf{x}, \mathbf{y}), (\mathbf{x}', \mathbf{y}') \in X \times Y$, let $A(\mathbf{x}, \mathbf{y}, \mathbf{x}', \mathbf{y}')$ such that*

$$A(\mathbf{x}, \mathbf{y}, \mathbf{x}', \mathbf{y}') = \frac{1}{\tau} D_X(\mathbf{x}, \mathbf{x}') + \frac{1}{\sigma} D_Y(\mathbf{y}, \mathbf{y}') - \langle \mathbf{K}(\mathbf{x} - \mathbf{x}'), \mathbf{y} - \mathbf{y}' \rangle.$$

Let a scalar $\Omega \geq 0$ and some step sizes τ, σ such that for all $(\mathbf{x}, \mathbf{y}), (\mathbf{x}', \mathbf{y}') \in X \times Y$,

$$0 \leq A(\mathbf{x}, \mathbf{y}, \mathbf{x}', \mathbf{y}') \leq \Omega. \quad (\text{B.2})$$

Consider running PDA on the associated min-max problem for T iterations. Consider weights $\omega_1, \dots, \omega_T$ and $S_T = \sum_{t=1}^T \omega_t$. Then we have the critical inequality: $\forall (\mathbf{x}, \mathbf{y}) \in X \times Y$,

$$\mathcal{L}^{\mathbf{K}}(\mathbf{x}^{t+1}, \mathbf{y}) - \mathcal{L}^{\mathbf{K}}(\mathbf{x}, \mathbf{y}^{t+1}) \leq A(\mathbf{x}, \mathbf{y}, \mathbf{x}^t, \mathbf{y}^t) - A(\mathbf{x}, \mathbf{y}, \mathbf{x}^{t+1}, \mathbf{y}^{t+1}). \quad (\text{B.3})$$

Additionally, summing up (B.3), we have, for all $(\mathbf{x}, \mathbf{y}) \in X \times Y$,

$$\sum_{t=1}^T \omega_t (\mathcal{L}^{\mathbf{K}}(\mathbf{x}^t, \mathbf{y}) - \mathcal{L}^{\mathbf{K}}(\mathbf{x}, \mathbf{y}^t)) \leq \omega_0 A[\mathbf{x}, \mathbf{y}, \mathbf{x}^0, \mathbf{y}^0] + \omega_T \Omega - \omega_1 \Omega - \omega_T A[\mathbf{x}, \mathbf{y}, \mathbf{x}^T, \mathbf{y}^T].$$

In particular, for $(\bar{\mathbf{x}}^T, \bar{\mathbf{y}}^T) = (1/S_T) \sum_{t=1}^T \omega_t (\mathbf{x}^t, \mathbf{y}^t)$, for all $(\mathbf{x}, \mathbf{y}) \in X \times Y$,

$$\mathcal{L}^{\mathbf{K}}(\bar{\mathbf{x}}^T, \mathbf{y}) - \mathcal{L}^{\mathbf{K}}(\mathbf{x}, \bar{\mathbf{y}}^T) \leq \sum_{t=1}^T \frac{\omega_t}{S_T} (\mathcal{L}^{\mathbf{K}}(\mathbf{x}^t, \mathbf{y}) - \mathcal{L}^{\mathbf{K}}(\mathbf{x}, \mathbf{y}^t))$$

and therefore

$$\mathcal{L}^{\mathbf{K}}(\bar{\mathbf{x}}^T, \mathbf{y}) - \mathcal{L}^{\mathbf{K}}(\mathbf{x}, \bar{\mathbf{y}}^T) \leq \Omega \frac{\omega_T}{S_T}.$$

We also prove the following lemma.

Lemma B.2. *Recall that*

$$L_{\mathbf{K}} = \sup_{\|\mathbf{x}\|_X \leq 1, \|\mathbf{y}\|_Y \leq 1} \langle \mathbf{K} \mathbf{x}, \mathbf{y} \rangle.$$

For $(\|\cdot\|_X, \|\cdot\|_Y) = (\|\cdot\|_2, \|\cdot\|_2)$, $L_{\mathbf{K}} = \lambda \|\mathbf{v}\|_2$.

For $(\|\cdot\|_X, \|\cdot\|_Y) = (\|\cdot\|_1, \|\cdot\|_1)$, $L_{\mathbf{K}} = \lambda \|\mathbf{v}\|_\infty$.

Proof. Recall that $\mathbf{K} : \mathbb{R}^A \rightarrow \mathbb{R}^{A \times S}$ is defined as, $\forall (\mathbf{x}, \mathbf{y}) \in \mathbb{R}^A \times \mathbb{R}^{A \times S}$,

$$\langle \mathbf{K} \mathbf{x}, \mathbf{y} \rangle = \lambda \sum_{a=1}^A x_a \mathbf{y}_a^\top \mathbf{v} = \lambda \sum_{a=1}^A \sum_{s'=1}^S x_a y_{as'} v_{s'}.$$

In particular, $K_{a's', a} = 1_{\{a=a'\}} \lambda v_{s'}, \forall a, a' \in \mathbb{A}, s' \in \mathbb{S}$.

1. ℓ_2 setup. By definition, $L_{\mathbf{K}}$ is the square root of maximum modulus of the eigenvalues of $\mathbf{K}^\top \mathbf{K} \in \mathbb{R}^{A \times A}$. Let $\mathbf{x} \in \mathbb{R}^A$. Then for $a' \in \mathbb{A}, s' \in \mathbb{S}$,

$$(\mathbf{K}\mathbf{x})_{a's'} = \lambda x_{a'} v_{s'}.$$

Therefore, by definition of matrix-vector product,

$$\begin{aligned} (\mathbf{K}^\top \mathbf{K}\mathbf{x})_a &= \sum_{a'', s''} (\mathbf{K}^\top)_{a, s'' a''} (\mathbf{K}\mathbf{x})_{s'' a''} = \sum_{a'', s''} (\mathbf{K}^\top)_{a, s'' a''} \lambda x_{a''} v_{s''} = \sum_{a'', s''} (\mathbf{K})_{s'' a'' a} \lambda x_{a''} v_{s''} \\ &= \sum_{a'', s''} 1_{\{a=a''\}} \lambda v_{s''} \lambda x_{a''} v_{s''} = \lambda^2 \left(\sum_{s'' \in \mathbb{S}} v_{s''}^2 \right) x_a = \lambda^2 \|\mathbf{v}\|_2^2 x_a. \end{aligned}$$

This directly implies that $L_{\mathbf{K}} = \lambda \|\mathbf{v}\|_2$.

2. ℓ_1 setup. This is straightforward from the definition of \mathbf{K} , the definition $L_{\mathbf{K}} = \sup_{\|\mathbf{x}\|_X \leq 1, \|\mathbf{y}\|_Y \leq 1} \langle \mathbf{K}\mathbf{x}, \mathbf{y} \rangle$, as well as the fact that $\mathbf{v} \geq \mathbf{0}$.

□

C Proof of Theorem 3.1

Our proof proceeds in several steps. We first show how to choose an upper bound Ω and step-sizes σ, τ uniformly across all epochs. We then show that the duality gap $\max_{\mathbf{y} \in \mathbb{P}_s} F^{\bar{\mathbf{x}}^T, \mathbf{y}}(\mathbf{v}^*) - \min_{\mathbf{x} \in \Delta(A)} F^{\mathbf{x}, \bar{\mathbf{y}}^T}(\mathbf{v}^*)$ can be bounded by the sum of 5 terms e_1, \dots, e_5 . We then give the dependency of e_1, \dots, e_5 in terms of T the number of PD iterations.

Upper bound Ω and step sizes σ, τ . Our goal here is to define a scalar Ω common across all epochs of Algorithm 1. Note that for a given matrix \mathbf{K} and some step sizes σ, τ , the scalar Ω is defined as satisfying (B.2). From Remark 2 of Chambolle and Pock [2016], a possible choice for Ω is

$$\Omega = 2(\Theta_X/\tau + \Theta_Y/\sigma) \quad (\text{C.1})$$

as soon as

$$\frac{1}{\sigma} \frac{1}{\tau} \geq L_{\mathbf{K}}^2 \quad (\text{C.2})$$

Therefore, we want to find σ, τ such that (C.2) holds for any matrix \mathbf{K} visited by our algorithm. We then define Ω as in (C.1).

Note that Lemma B.2 gives the value of $L_{\mathbf{K}}$ for the ℓ_1 and the ℓ_2 setup. A naive choice of step sizes is then simply $\sigma = \tau = L_{\mathbf{K}}^{-1}$. However, a better choice is one where $\Theta_X/\tau = \Theta_Y/\sigma$, since Ω , defined in (C.1), will appear in our upper bound on the error of our algorithm. Under the condition (C.2), we can choose $\tau = \left(\sqrt{\Theta_X/\Theta_Y}\right) L_{\mathbf{K}}^{-1}$ and $\sigma = L_{\mathbf{K}}^{-2} \tau^{-1}$. Note that this *asymmetric* choice of step sizes essentially accounts for the difference in dimension between the space $\Delta(A)$ of x and the space $\mathbb{P}_s \subset (\Delta(S))^A \subset \mathbb{R}^{A \times S}$ of y .

The exact values of σ, τ in terms of S, A are not needed here, as long as (C.2) is satisfied for all matrix \mathbf{K} visited by our algorithm. Since $L_{\mathbf{K}}$ changes in the ℓ_1 or ℓ_2 setup and in order to keep a convergence rate independent of the choice of the proximal setup here, we defer giving the exact values of σ, τ to Appendix E.3.

Bounding the duality gap. Recall the definition of $\mathcal{L}^{\mathbf{K}}$ as in (B.1). Let us focus on the error for $s \in \mathbb{S}$. Then

$$\mathcal{L}^{\mathbf{K}^*}(\bar{\mathbf{x}}^T, \mathbf{y}) - \mathcal{L}^{\mathbf{K}^*}(\mathbf{x}, \bar{\mathbf{y}}^T) \quad (\text{C.3})$$

$$\begin{aligned} &\leq \frac{1}{S_T} \left(\sum_{\ell=1}^k \sum_{t=\tau_\ell}^{\tau_\ell+T_\ell} \omega_t (\mathcal{L}^{\mathbf{K}^*}(\mathbf{x}^t, \mathbf{y}) - \mathcal{L}^{\mathbf{K}^*}(\mathbf{x}, \mathbf{y}^t)) \right) \\ &\leq \frac{1}{S_T} \left(\sum_{\ell=1}^k \sum_{t=\tau_\ell}^{\tau_\ell+T_\ell} \omega_t (\mathcal{L}^{\mathbf{K}^\ell}(\mathbf{x}^t, \mathbf{y}) - \mathcal{L}^{\mathbf{K}^\ell}(\mathbf{x}, \mathbf{y}^t)) \right) \quad (\text{C.4}) \end{aligned}$$

$$+ \frac{1}{S_T} \left(\sum_{\ell=1}^k \sum_{t=\tau_\ell}^{\tau_\ell+T_\ell} \omega_t (\mathcal{L}^{\mathbf{K}^*-\mathbf{K}^\ell}(\mathbf{x}^t, \mathbf{y}) - \mathcal{L}^{\mathbf{K}^*-\mathbf{K}^\ell}(\mathbf{x}, \mathbf{y}^t)) \right). \quad (\text{C.5})$$

Bounds on (C.4). Let us first focus on the term at (C.4). By applying Proposition B.1, we obtain

$$\frac{1}{S_T} \left(\sum_{\ell=1}^k \sum_{t=\tau_\ell}^{\tau_\ell+T_\ell} \omega_t (\mathcal{L}^{\mathbf{K}^\ell}(\mathbf{x}^t, \mathbf{y}) - \mathcal{L}^{\mathbf{K}^\ell}(\mathbf{x}, \mathbf{y}^t)) \right) \quad (\text{C.6})$$

$$= \frac{1}{S_T} \left(\sum_{\ell=1}^k \sum_{t=\tau_\ell}^{\tau_\ell+T_\ell} (\omega_{t+1} - \omega_t) (A^{\mathbf{K}^\ell}(\mathbf{x}, \mathbf{y}, \mathbf{x}^t, \mathbf{y}^t)) \right) \\ \leq \frac{1}{S_T} \omega_T \Omega + \frac{1}{S_T} \sum_{\ell=1}^k \omega_{\tau_\ell} \mathcal{L}^{\mathbf{K}^\ell - \mathbf{K}^{\ell-1}}(\mathbf{x} - \mathbf{x}^t, \mathbf{y} - \mathbf{y}^t) \quad (\text{C.7})$$

$$\leq \frac{1}{S_T} \omega_T \Omega + \frac{4R_X R_Y}{S_T} \sum_{\ell=1}^k \omega_{\tau_\ell} L_{\mathbf{K}^\ell - \mathbf{K}^{\ell-1}} \\ \leq \frac{1}{S_T} \omega_T \Omega + \frac{4R_X R_Y C}{S_T} \sum_{\ell=1}^k \omega_{\tau_\ell} \|\mathbf{v}^\ell - \mathbf{v}^{\ell-1}\|_\infty \quad (\text{C.8})$$

$$\leq \frac{1}{S_T} \omega_T \Omega \\ + \frac{4R_X R_Y C}{S_T} \sum_{\ell=1}^k \omega_{\tau_\ell} \lambda^\ell (\|\mathbf{v}^1 - \mathbf{v}^0\|_\infty) \quad (\text{C.9})$$

$$+ \sum_{t=0}^{\ell-1} \left(\frac{\Omega_t}{T_t} + \frac{\Omega_{t-1}}{T_{t-1}} \right) \frac{1}{\lambda^t} \quad (\text{C.10})$$

$$\leq \frac{1}{S_T} \omega_T \Omega + \frac{4err_{1,0} R_X R_Y C}{S_T} \sum_{\ell=1}^k \omega_{\tau_\ell} \lambda^\ell \\ + \frac{4R_X R_Y \Omega C}{S_T} \sum_{\ell=1}^k \omega_{\tau_\ell} \lambda^\ell \left(\sum_{t=0}^{\ell-1} \left(\frac{1}{T_t} + \frac{1}{T_{t-1}} \right) \frac{1}{\lambda^t} \right) \\ \leq e_1 + e_2 + e_3, \quad (\text{C.11})$$

where $C = 1$ in the ℓ_1 setup and $C = \sqrt{S}$ in the ℓ_2 setup, where (C.7) follows from telescoping, (C.8) follows from Lemma (B.2). Inequality (C.10) follows from Proposition A.3 and $\epsilon_t = O(\Omega_\ell/T_\ell)$ in Proposition B.1, and

$$e_1 = \frac{1}{S_T} \omega_T \Omega, e_2 = \frac{4err_{1,0} R_X R_Y C}{S_T} \sum_{\ell=1}^k \omega_{\tau_\ell} \lambda^\ell, \\ e_3 = \frac{4R_X R_Y \Omega C}{S_T} \sum_{\ell=1}^k \omega_{\tau_\ell} \lambda^\ell \left(\sum_{t=0}^{\ell-1} \left(\frac{1}{T_t} + \frac{1}{T_{t-1}} \right) \frac{1}{\lambda^t} \right).$$

Bounds on (C.5). Note that

$$\frac{1}{S_T} \left(\sum_{\ell=1}^k \sum_{t=\tau_\ell}^{\tau_\ell+T_\ell} \omega_t (\mathcal{L}^{\mathbf{K}^* - \mathbf{K}^\ell}(\mathbf{x}^t, \mathbf{y}) - \mathcal{L}^{\mathbf{K}^* - \mathbf{K}^\ell}(\mathbf{x}, \mathbf{y}^t)) \right) \leq \frac{2R_X R_Y}{S_T} \left(\sum_{\ell=1}^k L_{\mathbf{K}^* - \mathbf{K}^\ell} \cdot \left(\sum_{t=\tau_\ell}^{\tau_\ell+T_\ell} \omega_t \right) \right).$$

Note that by Lemma B.2 we have $L_{\mathbf{K}^* - \mathbf{K}^\ell} \leq C \|\mathbf{v}^* - \mathbf{v}^\ell\|_\infty$ and from Proposition A.3 we have

$$\|\mathbf{v}^\ell - \mathbf{v}^*\|_\infty \leq \lambda^\ell \|\mathbf{v}^0 - \mathbf{v}^*\|_\infty + \lambda^\ell \sum_{t=1}^{\ell-1} \frac{\Omega_t}{T_t \lambda^t}$$

where the ϵ_t is replaced by Ω_t/T_t , the precision attained after T_t steps of PDA with payoff matrix \mathbf{K}^t . This implies that we can have the following upper bound:

$$L_{\mathbf{K}^\ell - \mathbf{K}^*} \leq C \lambda^\ell \|\mathbf{v}^0 - \mathbf{v}^*\|_\infty + C \lambda^\ell \sum_{t=1}^{\ell-1} \frac{\Omega_t}{T_t \lambda^t}.$$

Overall, (C.5) satisfies

$$\begin{aligned} \frac{1}{S_T} \left(\sum_{\ell=1}^k \sum_{t=\tau_\ell}^{\tau_\ell+T_\ell} \omega_t (\mathcal{L}^{\mathbf{K}^*-\mathbf{K}^\ell}(\mathbf{x}^t, \mathbf{y}) - \mathcal{L}^{\mathbf{K}^*-\mathbf{K}^\ell}(\mathbf{x}, \mathbf{y}^t)) \right) &\leq \frac{2R_X R_Y C}{S_T} \sum_{\ell=1}^k \left(\sum_{t=\tau_\ell}^{\tau_\ell+T_\ell} \omega_t \right) \cdot \left(\lambda^\ell \text{err}_0 + \lambda^\ell \sum_{t=1}^{\ell-1} \frac{\Omega_t}{T_t \lambda^t} \right) \\ &\leq e_4 + e_5, \end{aligned}$$

where

$$\begin{aligned} e_4 &= \frac{2\text{err}_{*,0} R_X R_Y C}{S_T} \sum_{\ell=1}^k \lambda^\ell \cdot \left(\sum_{t=\tau_\ell}^{\tau_\ell+T_\ell} \omega_t \right), \\ e_5 &= \frac{2R_X R_Y \Omega C}{S_T} \sum_{\ell=1}^k \lambda^\ell \left(\sum_{t=1}^{\ell-1} \frac{1}{T_t \lambda^t} \right) \cdot \left(\sum_{t=\tau_\ell}^{\tau_\ell+T_\ell} \omega_t \right). \end{aligned}$$

The term e_1 is the upper bound that we would obtain if we had known the matrix $\mathbf{K}^* = \mathbf{K}[\mathbf{v}^*]$ from the start. The e_2 term comes from updating the value vector \mathbf{v}^ℓ to $\mathbf{v}^{\ell+1}$ at the end of the epoch ℓ . The e_3 term comes from $\mathbf{v}^{\ell+1}$ being only an $O(1/T_\ell)$ approximation of $F(\mathbf{v}^\ell)$. The e_4 and e_5 terms are related to the error between \mathbf{v}^ℓ and \mathbf{v}^* .

We emphasize the importance of warm-starting for Algorithm 1. Crucially, by warm-starting the PDA algorithm at VI epoch $\ell + 1$ using the last iterate of the PDA algorithm at VI epoch ℓ , we are able maintain a telescopic sum from $t = 0$ to $T = T_1 + \dots + T_k$. Without warm-starts, we would end up with k independent telescopic sums (one per VI epoch). This would give an e_1 term of $(\sum_{\ell=1}^k \omega_{\tau_\ell+T_\ell}) \Omega/S_T$ which is significantly worse than $\omega_T \Omega/S_T$, the e_1 term of Proposition 3.1.

Convergence rates in terms of T We now investigate the convergence rate of the terms e_1, \dots, e_5 in terms of the number of PD iterations T . We have the following lemma. For the sake of clarity, we hide in the $O(\cdot)$ notation any dependency on S and A (i.e. on R_X, R_Y, Ω).

Lemma C.1. *Let $p, q \in \mathbb{N}$. At time step $t \geq 0$, let $\omega_t = t^p, T_\ell = \ell^q$. Then $\tau_\ell = O(\ell^{q+1}), T = O(k^{q+1}), S_T = O(k^{(p+1)(q+1)})$. Moreover,*

$$\begin{aligned} e_1 &= O\left(\frac{1}{T}\right), e_2 = O\left(\frac{\lambda^{T^{1/(q+1)}}}{T}\right), e_3 = O\left(\frac{1}{T^{2q/(q+1)}}\right), \\ e_4 &= O\left(\frac{\lambda^{T^{1/(q+1)}}}{T^{1/(q+1)}}\right), e_5 = O\left(\frac{1}{T^{q/(q+1)}}\right). \end{aligned}$$

Proof. Let $\omega_t = t^p, T_\ell = \ell^q$, for $t \geq 1$ and $p, q \in \mathbb{N}$. We have

$$\begin{aligned} T &= \sum_{\ell=1}^k T_\ell = \sum_{\ell=1}^k \ell^q = k^{q+1}, \\ \tau_\ell &= \sum_{i=1}^{\ell} T_i \ell^{q+1}, \\ S_T &= \sum_{t=1}^T \omega_t = \sum_{t=1}^{k^{q+1}} t^p = k^{(q+1)(p+1)} = T^{p+1}. \end{aligned}$$

For the sake of readability in the next bounds we hide the $O(\cdot)$ notations.

Bounds on e_1 . We have

$$e_1 = \frac{\omega_T}{S_T} = \frac{T^p}{T^{p+1}} = \frac{1}{T}.$$

Bounds on e_2 . We have

$$e_2 = \frac{1}{T^{p+1}} \sum_{\ell=1}^k \tau_\ell^p \lambda^\ell = \frac{1}{T^{p+1}} \sum_{\ell=1}^k \ell^{p(q+1)} \lambda^\ell = \frac{1}{T^{p+1}} k^{p(q+1)} \lambda^k = \frac{1}{T^{p+1}} T^p \lambda^{T^{1/(q+1)}} = \frac{\lambda^{T^{1/(q+1)}}}{T}.$$

Bounds on e_3 . We have

$$e_3 = \frac{1}{k^{(p+1)(q+1)}} \sum_{\ell=1}^k \ell^{p(q+1)} \lambda^\ell \frac{1}{\ell^q \lambda^\ell} = \frac{1}{k^{(p+1)(q+1)}} \sum_{\ell=1}^k \ell^{p(q+1)-q} = \frac{1}{k^{(p+1)(q+1)}} k^{p(q+1)-q+1} = \frac{1}{k^{2q}} = \frac{1}{T^{2q/(q+1)}}.$$

Bounds on e_4 . First we need to compute the term $\sum_{t=\tau_\ell}^{\tau_\ell+T_\ell} \omega_t$. We have

$$\begin{aligned} \sum_{t=\tau_\ell}^{\tau_\ell+T_\ell} \omega_t &= \sum_{t=\ell^{q+1}}^{\ell^{q+1}+\ell^q} t^p = \sum_{t=0}^{\ell^q} (\ell^{q+1} + t)^p = \sum_{t=0}^{\ell^q} \sum_{u=0}^p \binom{p}{u} \ell^{u(q+1)} t^{p-u} = \sum_{u=0}^p \binom{p}{u} \ell^{u(q+1)} \sum_{t=0}^{\ell^q} t^{p-u} \\ &= \sum_{u=0}^p \binom{p}{u} \ell^{u(q+1)} (\ell^q)^{p-u+1} = \sum_{u=0}^p \binom{p}{u} \ell^{uq+u+qp-qu+q} = \sum_{u=0}^p \binom{p}{u} \ell^{u+(p+1)q} = \ell^{(p+1)q} \sum_{u=0}^p \binom{p}{u} \ell^u \\ &= \ell^{(p+1)q} (1 + \ell)^p = \ell^{(p+1)q+p} = \ell^{(p+1)(q+1)-1}. \end{aligned}$$

Now we have

$$e_4 = \frac{1}{k^{(p+1)(q+1)}} \sum_{\ell=1}^k \lambda^\ell \ell^{(p+1)(q+1)-1} = \frac{1}{k^{(p+1)(q+1)}} \lambda^k k^{(p+1)(q+1)-1} = \frac{\lambda^k}{k} = \frac{\lambda^{T^{1/(q+1)}}}{T^{1/(q+1)}}.$$

Bounds on e_5 . Let us bound e_5 .

$$\begin{aligned} e_5 &= \frac{1}{k^{(p+1)(q+1)}} \sum_{\ell=1}^k \lambda^\ell \frac{1}{\ell^q \lambda^\ell} \ell^{(p+1)(q+1)-1} = \frac{1}{k^{(p+1)(q+1)}} \sum_{\ell=1}^k \ell^{pq+p} \\ &= \frac{1}{k^{(p+1)(q+1)}} k^{pq+p+1} = \frac{1}{k^q} = \frac{1}{T^{q/(q+1)}}. \end{aligned}$$

□

Theorem 3.1 follows directly from the previous lemma and our bound involving e_1, \dots, e_5 .

D Proof of Proposition 3.2

Let $B_2(\mathbf{y}_0, \alpha) = \{\mathbf{y} \in \mathbb{R}^{A \times S} \mid \frac{1}{2} \|\mathbf{y} - \mathbf{y}_0\|_2^2 \leq \alpha\}$.

D.1 ℓ_2 setup for y

The proximal update for y becomes

$$\begin{aligned} \min \langle \mathbf{y}_s, \mathbf{d}_s \rangle + \frac{1}{2\sigma} \|\mathbf{y} - \mathbf{y}'\|_2^2 \\ \mathbf{y} = (\mathbf{y}_a)_{a \in \mathbb{A}} \in (\Delta(S))^A, \\ \mathbf{y} \in B_2(\mathbf{y}_0, \alpha). \end{aligned}$$

Introduce Lagrange multiplier for ball constraint. Let us write the Lagrangian function $F(\mathbf{y}, \mu)$, where we introduce a Lagrangian multiplier $\mu \geq 0$ for the ball constraint, but we leave the simplex constraint unchanged:

$$F(\mathbf{y}, \mu) = \langle \mathbf{y}_s, \mathbf{d}_s \rangle + \frac{1}{2\sigma} \|\mathbf{y} - \mathbf{y}'\|_2^2 + \frac{\mu}{2} (\|\mathbf{y} - \mathbf{y}_0\|_2^2 - 2\alpha).$$

Let us show that we can compute $\arg \min_{\mathbf{y} \in (\Delta(S))^A} F(\mathbf{y}, \mu)$ in complexity $O(AS \log(S))$. Indeed,

$$\arg \min_{\mathbf{y} \in (\Delta(S))^A} F(\mathbf{y}, \mu) = \arg \min_{\mathbf{y} \in (\Delta(S))^A} \frac{1}{2} \left\| \mathbf{y} - \frac{\sigma}{1 + \sigma\mu} \left(\frac{1}{\sigma} \mathbf{y}' + \mu \mathbf{y}_0 - \mathbf{d} \right) \right\|_2^2.$$

Therefore, we can reduce $\arg \min_{\mathbf{y} \in (\Delta(S))^A} F(\mathbf{y}, \mu)$ to solving A Euclidean projections on the simplex $\Delta(S)$. Each Euclidean projection on the simplex $\Delta(S)$ can be done in $O(S \log(S))$ [Duchi et al., 2008].

Binary search for optimal Lagrange multiplier μ^* . Note that by definition, $q : \mu \mapsto F(\mathbf{x}^*(\mu), \mu)$ is a concave function on \mathbb{R}_+ . Therefore, if we have an upper bound $\bar{\mu}$ on μ^* an optimal Lagrange multiplier, we can binary search the interval $[0, \bar{\mu}]$ to find a maximum of q .

Upper bound on the Lagrange multiplier. Note that

$$\begin{aligned} q(\mu) &= -\mu\alpha + \min_{\mathbf{y} \in (\Delta(S))^A} \langle \mathbf{y}, \mathbf{d} \rangle + \frac{1}{2\sigma} \|\mathbf{y} - \mathbf{y}'\|_2^2 + \frac{\mu}{2} \|\mathbf{y} - \mathbf{y}_0\|_2^2 \\ &\leq -\mu\alpha + \langle \mathbf{y}_0, \mathbf{d} \rangle + \frac{1}{2\sigma} \|\mathbf{y}_0 - \mathbf{y}'\|_2^2. \end{aligned} \quad (\text{D.1})$$

Note that $q : \mu \mapsto q(\mu)$ is concave on \mathbb{R}^+ . Therefore if we found $\bar{\mu}$ such that $q(\bar{\mu}) \leq q(0)$, we can claim that $\mu^* \in [0, \bar{\mu}]$, where μ^* attains the maximum of q . Using our upper bound (D.1) on $q(\cdot)$ we know that we can choose any $\bar{\mu}$ such that $-\mu\alpha + \langle \mathbf{y}_0, \mathbf{d} \rangle + \frac{1}{2\sigma} \|\mathbf{y}_0 - \mathbf{y}'\|_2^2 \leq q(0)$, i.e. we choose an upper bound $\bar{\mu}$ as

$$\bar{\mu} = \frac{1}{\alpha} \left(\langle \mathbf{y}_0, \mathbf{d} \rangle + \frac{1}{2\sigma} \|\mathbf{y}_0 - \mathbf{y}'\|_2^2 - q(0) \right).$$

D.2 ℓ_1 setup for y

Let us fix $\beta \in \mathbb{R}$. For $\mathbf{d}' \in \mathbb{R}^{A \times S}$, $d'_{as'} = d_{as'} - (\beta/\sigma) \log(y'_{as'})$, we can write the proximal update as

$$\begin{aligned} \arg \min_{\mathbf{y}} \quad & \langle \mathbf{y}, \mathbf{d}'_s \rangle + \frac{\beta}{\sigma} \sum_{a=1}^A \sum_{s'=1}^S y_{as'} \log y_{as'} \\ \mathbf{y} &= (\mathbf{y}_a)_{a \in \mathbb{A}} \in (\Delta(S))^A, \\ \mathbf{y} &\in B_2(\mathbf{y}_0, \alpha). \end{aligned} \quad (\text{D.2})$$

Introduce Lagrange multiplier for ball constraint. Let us write the Lagrangian function $F(\mathbf{y}, \mu)$, where we introduce a Lagrange multiplier $\mu \geq 0$ for the ball constraint, but we leave the simplex constraint unchanged.

$$\begin{aligned} F(\mathbf{y}, \mu) &= \langle \mathbf{y}, \mathbf{d}'_s \rangle + \frac{\beta}{\sigma} \sum_{a=1}^A \sum_{s'=1}^S y_{as'} \log y_{as'} + \frac{\mu}{2} (\|\mathbf{y} - \mathbf{y}_0\|_2^2 - \alpha) \\ &= \sum_{a=1}^A \langle \mathbf{y}_a, \mathbf{d}'_{sa} \rangle + \frac{\beta}{\sigma} \sum_{s'=1}^S y_{as'} \log y_{as'} + \frac{\mu}{2} (\|\mathbf{y}_a - \mathbf{y}_{0,a}\|_2^2 - \alpha). \end{aligned}$$

The key observation is that $F(\mathbf{y}, \mu)$ is separable over the actions a . Therefore, in order to solve $\arg \min_{\mathbf{y} \in (\Delta(S))^A} F(\mathbf{y}, \mu)$ we can solve A subproblems, where for each $a = 1, \dots, A$ we solve the problem

$$\arg \min_{\mathbf{y}_a \in \Delta(S)} \langle \mathbf{y}_a, \mathbf{d}'_{sa} \rangle + \frac{\beta}{\sigma} \sum_{s'=1}^S y_{as'} \log y_{as'} + \frac{\mu}{2} (\|\mathbf{y}_a - \mathbf{y}_{0,a}\|_2^2 - \alpha). \quad (\text{D.3})$$

Introduce Lagrange multiplier for simplex constraint. We now introduce a further relaxation for each problem (D.3), by relaxing the simplex constraint using a Lagrange multiplier ν as follows:

$$\begin{aligned}
& \arg \min_{\mathbf{y}_a \geq 0} \langle \mathbf{y}_a, \mathbf{d}'_{sa} \rangle + \frac{\beta}{\sigma} \sum_{s'=1}^S y_{as'} \log y_{as'} + \frac{\mu}{2} (\|\mathbf{y}_a - \mathbf{y}_{0,a}\|_2^2 - \alpha) + \nu (\sum_{s'} y_{as'} - 1) \\
&= \arg \min_{\mathbf{y}_a \geq 0} \langle \mathbf{y}_a, \mathbf{d}'_{sa} + \nu \rangle + \frac{\beta}{\sigma} \sum_{s'=1}^S y_{as'} \log y_{as'} + \frac{\mu}{2} \|\mathbf{y}_a - \mathbf{y}_{0,a}\|_2^2 \\
&= \arg \min_{\mathbf{y}_a \geq 0} \frac{\beta}{\sigma} \sum_{s'=1}^S y_{as'} \log y_{as'} + \frac{\mu}{2} \|\mathbf{y}_a - \mathbf{y}_{0,a}\|_2^2 + \frac{1}{\mu} (\mathbf{d}'_{sa} + \nu) \|\mathbf{y}_a\|_2^2 \\
&= \arg \min_{\mathbf{y}_a \geq 0} \sum_{s'=1}^S y_{as'} \log y_{as'} + \frac{\sigma\mu}{2\beta} \|\mathbf{y}_a - \mathbf{y}_{0,a}\|_2^2 + \frac{1}{\mu} (\mathbf{d}'_{sa} + \nu) \|\mathbf{y}_a\|_2^2. \tag{D.4}
\end{aligned}$$

We now arrive at a problem that decomposes into simple variable-wise updates: the negative entropy proximal mapping. For each variable $y_{a's}$ the update (D.4) is known to be equal (Combettes and Pesquet [2011]) to

$$y_{as'} = \frac{\beta}{\sigma\mu} W \left(\frac{\sigma\mu}{\beta} \exp \left(\frac{\sigma\mu}{\beta} \left(y_{0,as'} - \frac{1}{\mu} (\mathbf{d}'_{sas'} + \nu) \right) - 1 \right) \right) \tag{D.5}$$

where W is the principal branch of the *Lambert W function*, which is defined as the inverse of $w \mapsto w \log w$. The inverse is unique for $w \in [0, \infty)$. This function is not simple, but it can be computed quickly, and has standard implementations in the major numerical computing languages (e.g. in SciPy). As a heuristic benchmark, evaluating $W(a)$, $a \in \mathbb{R}_{++}$ using SciPy takes about twice as long as evaluating $\exp(a)$ (using numpy libraries for all function evaluations), based on generating 1000 random numbers in $[0, 1000]$. Now we may find the appropriate ν^* such that the sum-to-one constraint is satisfied by binary search ν .

Binary search for ν^* . Let $\nu \in \mathbb{R}$ and $\mathbf{y}_a(\nu)$ the associated solution obtained from (D.5). If $\sum_{s'}^S y_a(\nu)_{s'} > 1$, then ν is a lower bound on ν^* . Similarly, if $\sum_{s'}^S y_a(\nu)_{s'} < 1$, then ν is an upper bound on ν^* . Since we know that $\nu^* > -\infty$, we can explore the set $\{-2^\ell \mid \ell \geq 0\}$ until we found a lower bound on ν^* . If in this set we also found ν such that $\sum_{s'}^S y_a(\nu)_{s'} > 1$ then we also obtain an upper bound on ν^* . Otherwise, we can explore the set $\{2^\ell \mid \ell \geq 0\}$ to find an upper bound on ν^* .

Finally we get that we can reduce $\arg \min_{\mathbf{y} \in (\Delta(S))^A} F(\mathbf{y}, \mu)$ to a problem that can be solved in $\log(1/\epsilon)$ time, when treating evaluations of the Lambert W function as a constant.

Now that we have a method for computing $\arg \min_{\mathbf{y} \in (\Delta(S))^A} F(\mathbf{y}, \mu)$, we can now binary search the Lagrange multiplier μ in order to find a feasible solution to (D.2).

Upper bound on μ^* . We know that $\mu^* \in [0, +\infty)$, where μ^* is an argmax of

$$q : \mu \mapsto \min_{\mathbf{y}_a \in \Delta(S)} \langle \mathbf{y}_a, \mathbf{d}_{sa} \rangle + \frac{\beta}{\sigma} KL(\mathbf{y}_a, \mathbf{y}'_a) + \mu (\|\mathbf{y}_a - \mathbf{y}_a^0\|_2^2 - \alpha).$$

- There is a closed form solution for $q(0)$ since this is the proximal update for the relative entropy.
- We know that

$$q(\mu) \leq -\mu\alpha + \langle \mathbf{y}_a^0, \mathbf{d}_{sa} \rangle + \frac{\beta}{\sigma} KL(\mathbf{y}_a^0, \mathbf{y}'_a).$$

- Therefore an upper bound $\bar{\mu}$ for μ^* is

$$\bar{\mu} = \frac{1}{\alpha} \left(\langle \mathbf{y}_a^0, \mathbf{d}_{sa} \rangle + \frac{\beta}{\sigma} KL(\mathbf{y}_a^0, \mathbf{y}'_a) - q(0) \right).$$

We can then perform a binary search for μ^* in $[0, \bar{\mu}]$ exactly as for the ℓ_2 setup.

Choice of the parameter β . Now we need to choose β such that ψ becomes strongly convex modulus 1. If we set $\beta = \frac{A}{2}$ then we get strong convexity modulus 1 with respect to the ℓ_1 norm. To show this, we use the second-order definition of strong convexity:

$$\langle \nabla^2 \psi(y)h, h \rangle \geq \|h\|_1^2, \forall y \in Y, h \in \mathbb{R}^{AS}$$

Taking an arbitrary $h \in \mathbb{R}^{AS}$ we get from Cauchy-Schwarz:

$$\begin{aligned} \left(\sum_a \sum_{s'} h_{as'} \right)^2 &= \sum_a \left(\sum_{s'} h_{as'} \right)^2 + \sum_{a,a'} \left(\sum_{s'} h_{as'} \right) \left(\sum_{s'} h_{a's'} \right) \\ &\leq \sum_a \frac{A}{2} \left(\sum_{s'} h_{as'} \right)^2 = \sum_a \frac{A}{2} \left(\sum_{s'} \frac{h_{as'}}{\sqrt{y_{as'}}} \sqrt{y_{as'}} \right)^2 \\ &\leq \sum_a \frac{A}{2} \|\sqrt{y_a}\|_2^2 \left(\sum_{s'} \frac{h_{as'}^2}{y_{as'}} \right)^2 = \sum_a \frac{A}{2} \left(\sum_{s'} \frac{h_{as'}^2}{y_{as'}} \right)^2, \end{aligned}$$

which shows strong convexity modulus 1 with respect to the ℓ_1 norm.

Remark D.1. It may be possible to choose a stronger constant β , following Juditsky et al. [2011], Chapter 5, pages 23-24. However, this would require to introduce a modified norm for element $(\mathbf{y}_{sa})_{a \in \mathbb{A}}$ of the set \mathbb{P}_s . We leave this (potential) improvement for future work.

E Details on the complexities of Theorem 3.5

E.1 Summary of proximal setups for ellipsoidal uncertainty sets

We first present a summary of the different sets and constants defined in this paper.

Sets.

1. $X = \Delta(A)$,
2. $Y = (\Delta(S))^A \cap B_2(\mathbf{y}_0, \alpha)$.

Diameter and complexities. We call R the maximum of the considered norm on the considered set Z : $R = \max_{z \in Z} \|z\|_Z$. We call Θ the maximum of the Bregman divergence D on the considered set Z : $\Theta = \max_{z, z' \in Z} D(z, z')$. The complexity of computing the proximal update up to ϵ is C_ϵ . We have:

1. For $\|\cdot\|_X = \|\cdot\|_1$:
 - $\psi_X = \text{entropy}$,
 - $R_X = O(1), \Theta_X = O(\log(A))$,
 - $comp_\epsilon = O(A)$.
2. For $\|\cdot\|_X = \|\cdot\|_2$:
 - $\psi_X = (1/2)\|\cdot\|_2^2$,
 - $R_X = O(1), \Theta_X = O(1)$,
 - $comp_\epsilon = O(A \log(A))$.
3. For $\|\cdot\|_Y = \|\cdot\|_1$:
 - $\psi_Y = \text{sum-entropy}$,
 - $R_Y = O(A), \Theta_Y = O(A^2 \log(S))$,
 - $comp_\epsilon = O(AS \log^2(\epsilon^{-1}))$.
4. For $\|\cdot\|_Y = \|\cdot\|_2$:
 - $\psi_Y = (1/2)\|\cdot\|_2^2$,
 - $R_Y = O(\sqrt{A}), \Theta_Y = O(A)$,
 - $comp_\epsilon = O(AS \log(S) \log(\epsilon^{-1}))$.

E.2 Convergence in terms of number of iterations

Note that the results of Theorem 3.5 follows from the rate in Theorem 3.1 and the value of $R_X, R_Y, \Theta_X, \Theta_Y$ given in the above section. Here we provide details of the convergence rate computation in the case $q = 2$.

E.3 Overall complexity analysis for $(\|\cdot\|_X, \|\cdot\|_Y) = (\|\cdot\|_1, \|\cdot\|_1)$

Step sizes For the ℓ_1 setup, following Lemma B.2, we have $L_{K^\ell} = \lambda\|v^\ell\|_\infty$, for any epoch ℓ . Note that at epoch ℓ , by construction, the vector v^ℓ corresponds to the reward obtained after ℓ periods by the sequence $(\bar{x}^{\tau^\ell}, \bar{y}^{\tau^\ell}, \dots, \bar{x}^0, \bar{y}^0)$. This implies that $\|v^\ell\|_\infty \leq r_\infty(1 - \lambda^{\ell+1})(1 - \lambda)^{-1} \leq r_\infty(1 - \lambda)^{-1}$, where $r_\infty = \max_{s,a} c_{sa}$. Therefore in the ℓ_1 setup we can choose

$$\begin{aligned}\tau &= \frac{1 - \lambda}{\lambda r_\infty A} \frac{\sqrt{\log(A)}}{\sqrt{\log(S)}}, \\ \sigma &= \frac{(1 - \lambda)A}{\lambda r_\infty} \frac{\sqrt{\log(A)}}{\sqrt{\log(S)}}, \\ \Omega &= 2A \sqrt{\frac{\log(S)}{\log(A)}} \frac{\lambda r_\infty}{1 - \lambda}.\end{aligned}$$

We combine the definitions of the terms e_1, \dots, e_5 from Proposition 3.1 (which includes the constants R, Θ, Ω and C) with the convergence rates of Proposition C.1. Since e_5 has the slowest convergence rate, we use this term to give the overall number of arithmetic operations for Algorithm 1 to return an ϵ -optimal solution to the robust MDP problem.

Convergence rate of PD. For $q = 2$, the error bounds of Proposition C.1 become:

$$\begin{aligned}e_1 &= O\left(\frac{A\sqrt{\log(S)}}{T\sqrt{\log(A)}}\right), e_2 = O\left(\frac{A\lambda^{T^{1/3}}}{T}\right), \\ e_3 &= O\left(\frac{A^2\sqrt{\log(S)}}{T^{4/3}\sqrt{\log(A)}}\right), e_4 = O\left(\frac{A^2\sqrt{\log(S)}\lambda^{T^{1/3}}}{T^{1/3}\sqrt{\log(A)}}\right), \\ e_5 &= O\left(\frac{A^2\sqrt{\log(S)}}{T^{2/3}\sqrt{\log(A)}}\right).\end{aligned}$$

Complexity of PD update. For each epoch $\ell = 1, \dots, k$, solving each proximal update with accuracy $\epsilon > 0$, the complexity of epoch ℓ is as follows.

$$\text{comp}_\ell = O\left((AS^2 \log^2(\epsilon^{-1})) T_{ell}\right).$$

The overall complexity after $T = T_1 + \dots + T_k$ iterations is

$$\text{comp} = O\left((AS^2 \log^2(\epsilon^{-1})) T\right).$$

Since the e_5 term is the slowest to converge, for $q = 2$ the number of arithmetic operations in order to obtain a ϵ -optimal pairs in the robust MDP problem is $O\left(A^4 S^2 \left(\frac{\log(S)}{\log(A)}\right)^{0.75} \log^2(\epsilon^{-1}) \epsilon^{-1.5}\right)$.

E.4 Overall complexity analysis for $(\|\cdot\|_X, \|\cdot\|_Y) = (\|\cdot\|_2, \|\cdot\|_2)$

Step sizes The same argument as in the ℓ_1 setup, along with the equivalence between $\|\cdot\|_2$ and $\|\cdot\|_\infty$ in \mathbb{R}^S , yields

$$\begin{aligned}\tau &= \frac{1-\lambda}{\lambda r_\infty \sqrt{A} \sqrt{S}}, \\ \sigma &= \frac{(1-\lambda)\sqrt{A}}{\lambda r_\infty \sqrt{S}}, \\ \Omega &= 2\sqrt{A}\sqrt{S} \frac{\lambda r_\infty}{1-\lambda}.\end{aligned}$$

Convergence rate of PD. The error bounds of Proposition C.1 become, for $q = 2$:

$$\begin{aligned}e_1 &= O\left(\frac{\sqrt{AS}}{T}\right), e_2 = O\left(\frac{\sqrt{AS}\lambda^{T^{1/3}}}{T}\right), e_3 = O\left(\frac{AS}{T^{4/3}}\right), \\ e_4 &= O\left(\frac{AS\lambda^{T^{1/3}}}{T^{1/3}}\right), e_5 = O\left(\frac{AS}{T^{2/3}}\right).\end{aligned}$$

Complexity of PD update. For each epoch $\ell = 1, \dots, k$, the complexity of epoch ℓ is as follows.

$$\text{comp}_\ell = O\left((SA \log(A) + AS^2 \log(S) \log(\epsilon^{-1})) T_{\text{ell}}\right).$$

The overall complexity after $T = T_1 + \dots + T_k$ iterations is

$$\text{comp} = O\left((SA \log(A) + AS^2 \log(S) \log(\epsilon^{-1})) T\right).$$

Typically, $\log(A) \leq S$, and we have $\text{comp} = O(AS^2 \log(S) \log(\epsilon^{-1})T)$. Therefore, for $q = 2$, the number of arithmetic operations in order to obtain a ϵ -optimal pairs in the robust MDP problem is $O(A^{2.5}S^{3.5} \log(S) \log(\epsilon^{-1})\epsilon^{-1.5})$.

F Kullback-Leibler uncertainty set

We present here our complexity result for the KL uncertainty set. Recall that the KL uncertainty set is defined as

$$\begin{aligned}\mathbb{P} &= \times_{s \in \mathbb{S}} \mathbb{P}_s, \\ \mathbb{P}_s &= \{(\mathbf{y}_{sa})_{a \in \mathbb{A}} \in (\Delta(S))^A \mid \sum_{a \in \mathbb{A}} KL(\mathbf{y}_{sa}, \mathbf{y}_{sa}^0) \leq \alpha\}.\end{aligned}$$

We now prove Proposition 3.3. As the proof follows closely the lines of the proofs for the proximal updates on the ellipsoidal uncertainty set, for the sake of conciseness we only present an outline here.

Proof. **ℓ_2 setup.** We introduce a Lagrange multiplier for the KL constraint, and the proximal update boils down to solving A subproblems, each consisting of optimizing the sum of a linear form, an entropy function and an ℓ_2 distance. This is equivalent to solving subproblems of the form (D.3). Therefore, the ℓ_2 proximal update for a KL uncertainty set can be approximated within accuracy ϵ in $O(AS \log^2(\epsilon^{-1}))$.

ℓ_1 setup. For the ℓ_1 setup, we can introduce a Lagrange multiplier for the KL constraint; the objective becomes separable into A subproblems, each requiring to optimize (over the simplex of size $\Delta(S)$) the sum of a linear form and two KL terms, which brings down to optimizing, over the simplex, the sum of a linear form and a KL term. This can be computed in closed-form, and the ℓ_2 proximal update boils down to a bisection search onto the Lagrange multiplier. Therefore, the ℓ_2 proximal update for a KL uncertainty set can be approximated within accuracy $O(AS \log(\epsilon^{-1}))$. \square

G Performance measures for our simulations

Computing (DG). In order to compute (DG) for a pair \mathbf{x}, \mathbf{y} , we need to evaluate $\max_{\mathbf{y}' \in \mathbb{P}} R(\mathbf{x}, \mathbf{y}')$ and $\min_{\mathbf{x}' \in \Pi} R(\mathbf{x}', \mathbf{y})$. Following Wiesemann et al. [2013], $\max_{\mathbf{y}' \in \mathbb{P}} R(\mathbf{x}, \mathbf{y}')$ can be computed by finding the fixed point of the following operator, which is a contraction of factor λ :

$$F^{\mathbf{x}}(\mathbf{v})_s = \max_{\mathbf{y}' \in \mathbb{P}} \sum_{a=1}^A x_{sa} (c_{sa} + \lambda \mathbf{y}'^\top \mathbf{v}), \forall s \in \mathbb{S}.$$

Moreover, computing $\min_{\mathbf{x}' \in \Pi} R(\mathbf{x}', \mathbf{y})$ is equivalent to solving the (nominal) MDP with fixed kernel $\mathbf{y} \in \mathbb{P}$. Following Puterman [1994], Chapter 6.3, this can be solved by iterating the following contraction of factor λ :

$$F^{\mathbf{y}}(\mathbf{v})_s = \min_{\mathbf{x}_s \in \Delta(A)} \sum_{a=1}^A x_{sa} (c_{sa} + \lambda \mathbf{y}^\top \mathbf{v}), \forall s \in \mathbb{S}.$$

Each of these iterative algorithms can be stopped as soon $\|\mathbf{v}^{\ell+1} - \mathbf{v}^\ell\|_\infty < 2\lambda\epsilon(1-\lambda)^{-1}$, which ensures ϵ -optimality of the current iterates [Puterman, 1994], Chapter 6.3.

We present in the next figure the running times to compute (DG), both with Algorithm VI and Algorithm AVI. In particular, we generate 10 random Garnet MDP instances (see simulation section in the main body and next section), some random policies in Π , kernels in \mathbb{P} and vectors in \mathbb{R}^S and we compute (DG). We present the logarithm of the average running times to obtain ϵ -approximations of the quantities of interest, for $\epsilon = 0.25$ and $\alpha = \sqrt{n_{branch} \times A}$. We present our results for $\lambda = 0.6$ in Figure 2a and for $\lambda = 0.8$ in Figure 2b. We notice that computing (DG) quickly becomes very expensive, even using Algorithm AVI.

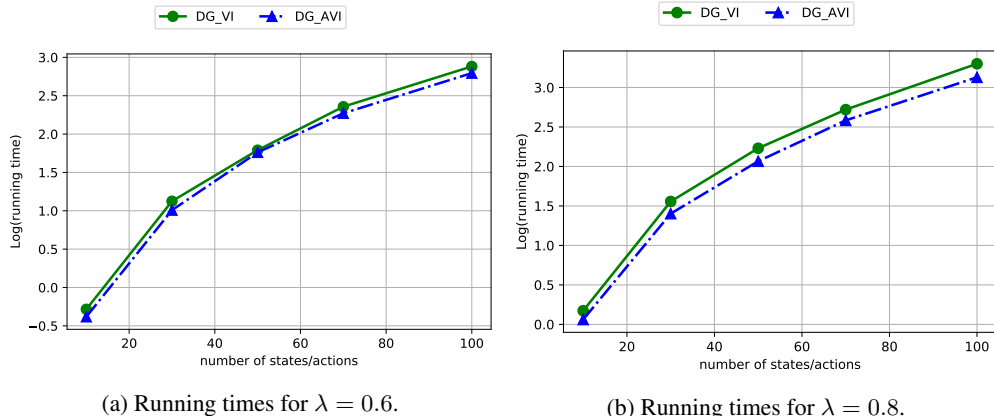


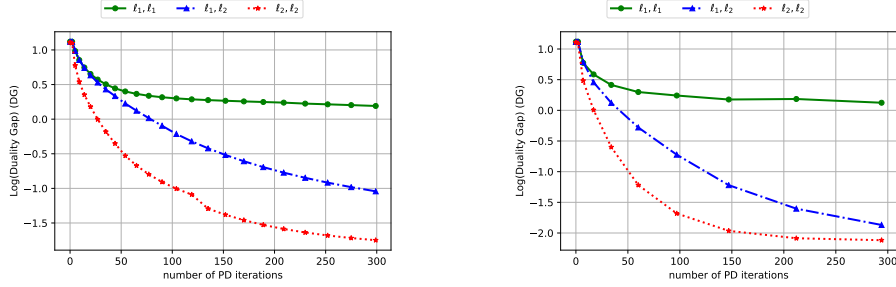
Figure 2: Average running time (s) to compute the duality gap of a Garnet MDP instance.

H Comparison of proximal setups for Algorithm 1

In this appendix we study the empirical performances of Algorithm 1, in order to identify the best one, which we will then compare to other VI approaches.

Empirical setup. All the simulations are implemented in Python 3.7.3, and were performed on a laptop with 2.2 GHz Intel Core i7 and 8 GB of RAM. We use Gurobi 8.1.1 to solve any linear or quadratic optimization problems involved. We generate Garnet MDPs (Archibald et al. [1995]), which are an abstract class of MDPs parametrized by a branching factor n_{branch} , equal to the number of reachable next states from each state-action pair (s, a) . We consider $n_{branch} = 0.5$ in our simulations. We draw the rewards parameters at random uniformly in $[0, 10]$. We fix a discount factor $\lambda = 0.8$. The radius α of the ℓ_2 ball from the uncertainty set (2.4) is set to $\alpha = \sqrt{n_{branch} \times A}$. All of the figures in this section show the logarithm of the performance measures (DG) in terms of the number of PD iteration performed in Algorithm 1. Apart from Figures 3a-3b, these performance measures are averaged across 10 randomly generated Garnet MDPs.

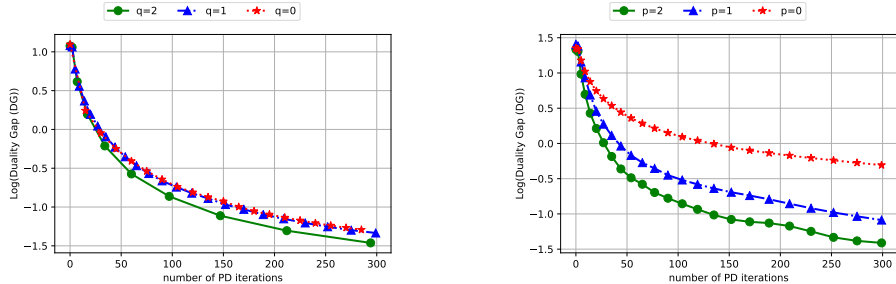
Impact of proximal setup. We fix $S, A = 30$ and we present in Figure 3a-3b the Duality Gap (DG) of the current weighted average of the iterates of our algorithm, for three different proximal setups $(\|\cdot\|_X, \|\cdot\|_Y) \in \{(\ell_1, \ell_1), (\ell_1, \ell_2), (\ell_2, \ell_2)\}$. The (ℓ_2, ℓ_2) setup performs the best, even though its theoretical guarantees are worse than the (ℓ_1, ℓ_1) setup (as seen in Theorem 3.5). This disparity between theory and practice is analogous to the case of stationary bilinear min-max problems [Gao et al., 2019]. In the rest of the simulations we focus on the (ℓ_2, ℓ_2) setup. Note that Figure 3a-3b shows performance for a single instance. This is because the (ℓ_1, ℓ_1) setup takes almost a day to run on a single instance of size $(S, A) = (30, 30)$ (compared to minutes for the (ℓ_2, ℓ_2) setup), most likely because of the two interwoven binary searches (see also Appendix D).



(a) Proximal setups comparison for $(p, q) = (1, 1)$. (b) Proximal setups comparison for $(p, q) = (2, 2)$.

Figure 3: Comparison of proximal setups for various proximal setups.

Impact of epoch scheme. We now investigate the impact of the epoch length $T_\ell = \ell^q$, parametrized by $q \in \mathbb{N}$. We fix $(S, A) = (30, 30)$ and we focus on the (ℓ_2, ℓ_2) setup. We fix the averaging scheme at $p = 1$ and we compare epoch lengths $q = 0, 1, 2$. The results are shown in Figure 4a. For the performance measure (DG), we find that $q = 0, q = 1$ and $q = 2$ yield comparable convergence rates (in terms of number of PD iterations), with $q = 2$ being slightly better than $q = 0, q = 1$ (note that our theory does not even guarantee convergence for $q = 0$). Note that for $q = 0$, our algorithm performs only one PD update at each epoch, before updating the value vector v , which has a cost of $O(AS^2)$. This may make $q = 0$ significantly slower in practice for large S, A , since the value vector updates have a negligible computational cost for $q > 0$ (compared to the numerous PD updates computational costs).



(a) (DG) in terms of number of PD iterations. (b) (DG) in terms of number of PD iterations.

Figure 4: Performances of our algorithm for various weights and epoch schemes.

Impact of weight scheme. We now investigate the impact of the weight scheme $\omega_t = t^p$ used to average iterates. We fix $(S, A) = (30, 30)$, $q = 2$ and use the (ℓ_2, ℓ_2) setup. We compare $p = 0, 1, 2$. Figure 4b shows that increasing averages ($p = 1, p = 2$) perform better than uniform average ($p = 0$), even though our convergence guarantees are independent of p . Similar observations have been made in zero-sum games and other convex-concave saddle-point problems [Gao et al., 2019].

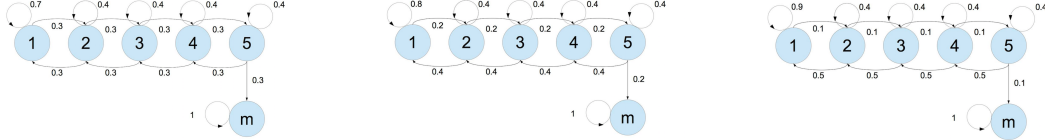
Remark H.1. In our simulations we set $\lambda = 0.8$. Of course, our algorithm works for any $\lambda \in (0, 1)$. However, the performance guarantees of Algorithm 1 may degrade for $\lambda \rightarrow 1$, as some of the constants in the $O(\cdot)$ notations of Theorem 3.5 depend on $1/(1 - \lambda)$, a situation similar to the complexity of Value Iteration VI. Moreover, when $\lambda \rightarrow 1$, computing the duality gap (DG) becomes very slow: computing the minimizer and maximizer requires iterating contraction mappings, each with improvement factor λ (see Appendix G). These last two limitations are not a particular shortcoming of our algorithm but are inherent to MDPs.

I MDP instance inspired from healthcare

We present here an example of the nominal kernel \mathbf{y}_0 of the healthcare MDP instance that we introduced in our simulation section. We show here an example with $S = 5$ health condition states and the mortality state. The state 1 corresponds to a healthy condition while $S = 5$ is more likely to lead to mortality. The transition kernel for general $S \geq 5$ are generated in the same fashion. In order to sample N kernels $\mathbf{y}_1, \dots, \mathbf{y}_N$ around the nominal transition \mathbf{y}_0 , we generate random Garnet MDPs $\tilde{\mathbf{y}}_1, \dots, \tilde{\mathbf{y}}_N$ with $n_{branch} = 20\%$ and we obtain N samples $\mathbf{y}_1, \dots, \mathbf{y}_N$ around \mathbf{y}_0 as

$$\mathbf{y}_i = 0.95 \cdot \mathbf{y}_0 + 0.05 \cdot \tilde{\mathbf{y}}_i, i = 1, \dots, N.$$

We choose the coefficients $(0.95, 0.05)$ in the above convex combination so that we obtain \mathbf{y}_i as small deviations from \mathbf{y}_0 .

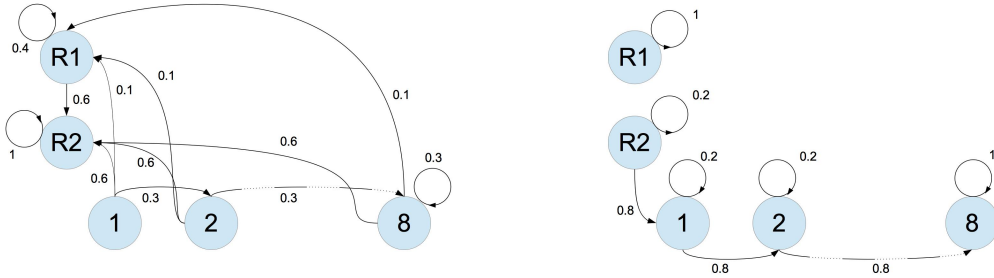


(a) Transition for action = *low drug level*. (b) Transition for action = *medium drug level*. (c) Transition for action = *high drug level*.

Figure 5: Transition rates for the healthcare MDP instance.

J Details on machine replacement example

We present here the nominal transition kernel \mathbf{y}_0 associated with the machine replacement example introduced in our numerical experiments section. Here we show an instance where there are 10 states: 8 states related to the condition of the machine, and two repair states. The instances for larger number of states are constructed in the same fashion by adding some condition states for the machine. To generate N samples around the nominal kernel \mathbf{y}_0 , we create small perturbations with Garnet MDP instances.



(a) Nominal transition for action = *repair* in our machine replacement MDP. (b) Nominal transition for action = *no repair* in our machine replacement MDP.

Figure 6: Transition rates for the machine replacement MDP instance.

K Details on numerical implementations

Value Iteration. At every epoch of Value Iteration VI, we need to compute $F(\mathbf{v})$ for the current value vector $\mathbf{v} \in \mathbb{R}^S$, where

$$F(\mathbf{v})_s = \min_{\mathbf{x}_s \in \Delta(A)} \max_{\mathbf{y}_s \in \mathbb{P}_s} \sum_{a=1}^A x_{sa} (c_{sa} + \lambda \cdot \mathbf{y}_{sa}^\top \mathbf{v}), \forall s \in \mathbb{S}.$$

In order to solve this program, we could use duality in the inner maximization program, and turn the computation of $F(\mathbf{v})_s$ into a large (minimization) convex program with linear objective, some constraints and a conic quadratic constraint (see Corollary 3 in Wiesemann et al. [2013]). However, we decide to take an alternate approach which results in a simpler optimization program, namely, a convex program with some linear constraints and a quadratic constraint. In particular, from convex duality we have, for any $s \in \mathbb{S}$,

$$\begin{aligned} F(\mathbf{v})_s &= \min_{\mathbf{x}_s \in \Delta(A)} \max_{\mathbf{y}_s \in \mathbb{P}_s} \sum_{a=1}^A x_{sa} (c_{sa} + \lambda \cdot \mathbf{y}_{sa}^\top \mathbf{v}) \\ &= \max_{\mathbf{y}_s \in \mathbb{P}_s} \min_{\mathbf{x}_s \in \Delta(A)} \sum_{a=1}^A x_{sa} (c_{sa} + \lambda \cdot \mathbf{y}_{sa}^\top \mathbf{v}). \end{aligned} \quad (\text{K.1})$$

Applying convex duality twice, we obtain

$$\begin{aligned} F(\mathbf{v})_s &= \max \mu \\ \mu &\in \mathbb{R}, \mathbf{y} \in \mathbb{P}_s, \\ c_{sa} + \lambda \mathbf{y}_{sa}^\top \mathbf{v} &\geq \mu, \forall a \in \mathbb{A}. \end{aligned} \quad (\text{K.2})$$

In our simulations, we use the formulation (K.2) in order to obtain the value of $F(\mathbf{v})_s$. Given the definition of \mathbb{P}_s as (2.4), formulation (K.1) is a linear program with linear constraints and one quadratic constraint. Following Ben-Tal and Nemirovski [2001], we can solve (K.2) up to accuracy ϵ in a number of arithmetic operations in $O(S^{3.5} A^{3.5} \log(1/\epsilon))$. We warm-start each of this optimization problem with the optimal solution found in the previous epoch of VI.

We would like to note that a priori, the optimal pair in $F(\mathbf{v})$ in the min-max formulation as in (2.1) may not be the same pair attaining the max-min formulation as in (K.1). However, we are only interested in the scalar value of $F(\mathbf{v})_s$, in order to run VI and obtain \mathbf{v}^* , the fixed-point of the operator T defined in (2.2). Once we have obtained the vector \mathbf{v}^* , we can eventually solve $F(\mathbf{v}^*)$ in its min-max form only once, in order to obtain the pair $(\mathbf{x}^*, \mathbf{y}^*)$ in $F(\mathbf{v}^*)$ in its min-max formulation. Alternately, the authors in Ho et al. [2018] provide a method to recover the optimal solution of the min-max problem (2.1) from the optimal solution of the max-min problem (K.1), in the case where \mathbb{P} is a weighted ℓ_1 ball centered around \mathbf{y}^0 .

Accelerated Value Iteration. Goyal and Grand-Clement [2018] interpret the vector $(\mathbf{I} - T)(\mathbf{v})$ as the gradient of some function at the vector \mathbf{v} . Adapting the acceleration scheme from convex optimization (Nesterov [1983, 2013]) to an accelerated iterative algorithm for computing \mathbf{v}^* leads to *Accelerated Value Iteration*, which significantly outperforms Value Iteration and variants when the discount factor is close to 1 [Goyal and Grand-Clement, 2018]. In particular, for any sequences of scalar $(\alpha_s)_{s \geq 0}$ and $(\gamma_s)_{s \geq 0} \in \mathbb{R}^{\mathbb{N}}$, Accelerated Value Iteration (AVI) is defined as

$$\mathbf{v}_0, \mathbf{v}_1 \in \mathbb{R}^S, \begin{cases} \mathbf{h}_t = \mathbf{v}_t + \gamma_t \cdot (\mathbf{v}_t - \mathbf{v}_{t-1}), \\ \mathbf{v}_{t+1} \leftarrow \mathbf{h}_t - \alpha_t (\mathbf{h}_t - T(\mathbf{h}_t)), \end{cases} \quad \forall t \geq 1. \quad (\text{AVI})$$

Following Goyal and Grand-Clement [2018], we choose step sizes as

$$\alpha_s = \alpha = 1/(1 + \lambda), \gamma_s = \gamma = (1 - \sqrt{1 - \lambda^2})/\lambda, \forall s \geq 1.$$

We use (K.2) in order to compute $F(\mathbf{h})$ for AVI.

Gauss-Seidel Value Iteration. We also consider Gauss-Seidel Value Iteration (GS-VI), a popular asynchronous variant of VI [Puterman, 1994], where $v_s^{t+1} = \max_{a \in \mathbb{A}} r_{sa} + \lambda \cdot \sum_{s'=1}^{s-1} P_{sas'} v_{s'}^{t+1} + \lambda \cdot \sum_{s'=s}^n P_{sas'} v_{s'}^t$.

Anderson Value Iteration. We also consider Anderson VI (referred to as *Anderson* in our figures), see Geist and Scherrer [2018]. In order to compute the next iterates \mathbf{v}^{t+1} , Anderson VI computes weights $\alpha_0, \dots, \alpha_m$ and updates \mathbf{v}^{t+1} as a linear combination of the last $(m + 1)$ -iterates $F(\mathbf{v}^t), \dots, F(\mathbf{v}^{t-m})$:

$$\mathbf{v}^{t+1} = \sum_{i=0}^m \alpha_i F(\mathbf{v}^{t-m+i}).$$

The weights $\alpha \in \mathbb{R}^{m+1}$ are updated at every iteration, see Algorithm 1 and Equation (1) in Geist and Scherrer [2018] for further details. There is no heuristics for choosing m ; we choose $m = 5$ in our numerical experiments.

L Numerical experiments for KL uncertainty set

We present here our numerical results for the KL uncertainty set. We consider the healthcare instance, the machine replacement instance and the random Garnet MDP instances, introduced in Section 4. The numerical setup is the same as for ellipsoidal uncertainty sets. Note that for the KL uncertainty set, we can not compare to Value Iteration directly, as there is no direct convex reformulation for the Bellman update

$$F(\mathbf{v}) = \min_{\mathbf{x} \in \Delta(A)} \max_{\substack{\sum_{a \in \mathbb{A}} x_a (r_{sa} + \lambda \mathbf{y}_{sa}^\top \mathbf{v}) \\ (\mathbf{y}_{sa}) \in (\Delta(S))^A, \\ \sum_{a \in \mathbb{A}} KL(\mathbf{y}_{sa}, \mathbf{y}_{sa}^0) \leq \alpha.}}$$

For a KL uncertainty set, computing a proximal update with the ℓ_1 setup requires one binary search, and computing a proximal update with the ℓ_2 setup requires two interwoven binary searches, as evidenced in Proposition 3.3. Therefore, we focus on the ℓ_1 setup for the y -player and the ℓ_1 setup for the x -player. We present the running times to compute an optimal policy on various instances below (healthcare and machine replacement examples, Garnet MDPs with high and low connectivity).

As the convergences times of our algorithm are longer for KL uncertainty sets than for ellipsoidal uncertainty sets, we only compute optimal solutions up to a number of states of 50. For the Garnet MDP instances, the number of actions is equal to the number of states, while there are two actions for the machine replacement instance and three actions for the healthcare instance.

Note that we also observe longer convergence rates for the (ℓ_1, ℓ_1) setup in Figures 3a-3b. Our FOM-VI algorithm finds a solution to the s -rectangular robust MDP problem with KL uncertainty sets but for the Garnet MDP instances the running time greatly increases, compared to the KL uncertainty sets. The running times for the more realistic healthcare and machine replacement instances also increase but remains below 100 seconds for up to 50 states.

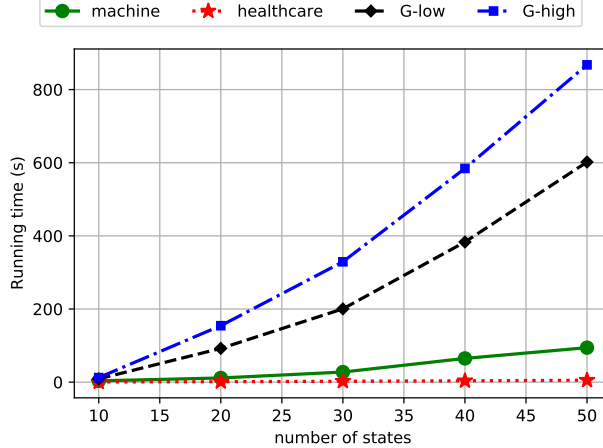


Figure 7: Performances of FOM-VI on four different instances for KL uncertainty sets.